

The effect of boundary conditions on the stability of two-dimensional flows in an annulus with permeable boundary

Konstantin Ilin*

Andrey Morgulis†

November 26, 2021

Abstract

We consider the stability of two-dimensional viscous flows in an annulus with permeable boundary. In the basic flow, the velocity has nonzero azimuthal and radial components, and the direction of the radial flow can be from the inner cylinder to the outer one or vice versa. In most earlier studies, all components of the velocity were assumed to be given on the entire boundary of the flow domain. Our aim is to study the effect of different boundary conditions on the stability of such flows. We focus on the following boundary conditions: at the inflow part of the boundary (which may be either inner or outer cylinder) all components of the velocity are known; at the outflow part of the boundary (the other cylinder), the normal stress and either the tangential velocity or the tangential stress are prescribed. Both types of boundary conditions are relevant to certain real flows: the first one - to porous cylinders, the second - to flows, where the fluid leaves the flow domain to an ambient fluid which is at rest. It turns out that both sets of boundary conditions make the corresponding steady flows more unstable (compared with earlier works where all components of the velocity are prescribed on the entire boundary). In particular, it is demonstrated that even the classical (purely azimuthal) Couette-Taylor flow becomes unstable to two-dimensional perturbations if one of the cylinders is porous and the normal stress (rather than normal velocity) is prescribed on that cylinder.

MSC Codes 76D05, 76E07

1 Introduction

In this paper we study the stability of steady two-dimensional viscous flows in an annulus between two permeable circular cylinders. In the basic flow, the velocity has nonzero azimuthal and radial components, and the direction of the radial flow can be from the inner cylinder to the outer one (the diverging flow) or from the outer cylinder to the inner one (the converging flow). The stability of viscous flows of this type has been studied by many authors (see Bahl , 1970; Min & Lueptow , 1994; Johnson & Lueptow , 1997; Kolyshkin & Vaillancourt , 1997; Kolesov & Shapakidze , 1999; Serre et al , 2008; Martinand et al , 2009; Gallet et al. , 2010; Fujita et al. , 1997; Kerswell , 2015; Martinand et al , 2017; Ilin & Morgulis , 2013, 2015, 2017, 2020). Most papers were motivated by applications to dynamic filtration devices (see, e.g., Wroński et al. , 1989; Beadoin & Jaffrin , 1989) and vortex flow reactors (see Giordano et al , 1998, and references therein). It was also argued by Gallet et al. (2010) and Kerswell (2015) that such flows may have some relevance to astrophysical flows in accretion discs (see also Kersale et al. , 2004). Similar inviscid flows have been also used as a model of a flow in the vaneless

*Department of Mathematics, University of York, Heslington, York YO10 5DD, UK. Email address for correspondence: konstantin.ilin@york.ac.uk

†Department of Mathematics, Mechanics and Computer Science, The Southern Federal University, Rostov-on-Don, and South Mathematical Institute, Vladikavkaz Center of RAS, Vladikavkaz, Russian Federation

diffuser of a radial pump (for references, see Tsujimoto et al , 1996; Ljevar et al , 2006; Guadagni et al , 2020).

In all these papers (except the ones on the flow in vaneless diffusers), all components of the velocity vector are prescribed on the permeable boundary of the flow domain. In what follows, these boundary conditions and the corresponding boundary-value problem will be called the *reference boundary condition* and the *reference problem*. It is widely accepted that these boundary conditions are appropriate for flows bounded by porous walls. This approach ignores the problem of modelling the flow in the porous medium and effectively assumes that this flow is given. Its big advantage is that one needs to study only the flow outside the porous medium. However, this also means that other boundary conditions may be relevant for flows bounded by porous walls, and it is known that in problems with permeable boundaries, the stability properties of a flow can be strongly affected by a change in boundary conditions (see Gallaire & Chomaz , 2004). It is therefore natural to raise the question: what is the effect of different boundary conditions on the stability of steady two-dimensional flows in an annulus with permeable boundary? The aim of the present paper is to answer this question for two sets of boundary conditions, both of which are different from the reference conditions.

We focus on the following boundary conditions. At the inflow part of the boundary (the flow inlet), which is either inner or outer cylinder, we specify all components of the velocity. At the outflow part (the flow outlet), represented by the other cylinder, the viscous normal stress in the free fluid is balanced by a given pressure in the porous wall and, in addition to that, either the tangential stress or the tangential velocity is prescribed. Since the normal stress contains the pressure, these two sets of boundary conditions will be referred to as the *pressure-stress* and *pressure-no-slip* conditions. Note that the only difference between the pressure-no-slip conditions and the reference conditions is that the condition for the normal velocity at the outlet is replaced with the condition for normal stress, while in the pressure-stress conditions the no-slip condition is also replaced with the condition for tangential stress. We argue in section 3 that both sets of boundary condition are no less relevant to real fluid flows than the reference conditions: the pressure-no-slip conditions - to flows between porous cylinders, the pressure-stress conditions - to flows in vaneless diffusers. Another reason to consider these conditions is that they appear in computational fluid dynamics as boundary conditions on artificial boundaries, used to obtain a finite computational domain for problems, originally formulated in infinite domains (see, e.g., Gresho , 1991; Heywood et al , 1996, and references there). In particular, both sets of conditions arise in a weak formulation of the Navier-Stokes equations (see Gunzburger , 1989, p. 61). Studies of the stability of flows bounded by artificial boundaries may shed some light of the upstream influence of boundary conditions imposed on such boundaries.

It turns out that, for both types of conditions at the outlet, the corresponding boundary-value problems formally reduce to the same inviscid problem for the Euler equations in the limit of high radial Reynolds number (based on the radial velocity at the inner cylinder and its radius). In the inviscid problem, the boundary conditions at the inlet remain the same (as those in the viscous problem), while only the pressure is prescribed at the outlet. This suggests that in both viscous problems, an inviscid instability, similar to that studied earlier (see Ilin & Morgulis , 2013; Kerswell , 2015), is likely to occur for sufficiently high radial Reynolds number.

For both types of viscous boundary conditions, we investigate the linear stability of the steady diverging and converging flows. Numerical calculations show that for high radial Reynolds numbers, the stability properties of the viscous flows are well described by the inviscid theory, while for small and moderate values of the radial Reynolds number the stability properties for both types of the outlet boundary conditions may be very different from what was found in Ilin & Morgulis (2015) for the reference problem. In particular, in the problem with the pressure-no-slip conditions, it turns out that both diverging and converging flows are unstable at arbitrarily small radial Reynolds numbers provided the azimuthal velocity at the inlet is much higher than the radial velocity. In this case, it is possible to construct an asymptotic approximation of the linear stability problem, which agrees with numerical

results. An interesting byproduct of this asymptotic approximation is that a particular case of the classical Couette-Taylor flow (with purely azimuthal basic flow), where one cylinder is impermeable (for the fluid) and rotating and the other one is permeable and stationary, turns out to be unstable to two-dimensional perturbations provided the normal stress condition (instead of the normal velocity condition) at the outer cylinder is imposed. This is strikingly different from the classical Couette-Taylor flow which is stable to two-dimensional perturbations. Another unexpected result, valid for both types of boundary conditions, is that there are flow regimes where the converging flows are unstable even if the azimuthal velocity at the inlet is zero.

The paper is organised as follows. In section 2, the inviscid problem is considered. The effects of viscosity are analysed in section 3. Section 4 contains the discussion of the results.

2 Inviscid problem

2.1 Formulation of the problem

We consider two-dimensional inviscid incompressible flows in an annulus between two concentric circles with radii r_1 and r_2 ($r_2 > r_1$). The circles are permeable for the fluid and there is a constant area flux $2\pi Q$ of the fluid through the annulus. We shall call the flow *diverging* if the fluid is pumped into the annulus at the inner circle and taken out at the outer circle and *converging* if the flow direction is reversed (i.e. the fluid enters the annulus at the outer circle and leaves it at the inner one). Quantity Q is positive for the diverging flow and negative for the converging flow. For later use, we define the parameter

$$\beta = \frac{Q}{|Q|},$$

so that $\beta = 1$ for the converging flow and $\beta = -1$ for the diverging flow.

Suppose that r_1 is taken as a length scale, $r_1^2/|Q|$ as a time scale, $|Q|/r_1$ as a scale for the velocity and $\rho Q^2/r_1^2$ for the pressure where ρ is the fluid density. Then the two-dimensional Euler equations, written in non-dimensional variables, have the form

$$u_t + uu_r + \frac{v}{r}u_\theta - \frac{v^2}{r} = -p_r, \quad (2.1)$$

$$v_t + uv_r + \frac{v}{r}v_\theta + \frac{uv}{r} = -\frac{1}{r}p_\theta, \quad (2.2)$$

$$\frac{1}{r}(ru)_r + \frac{1}{r}v_\theta = 0. \quad (2.3)$$

Here (r, θ) are the polar coordinates, u and v are the radial and azimuthal components of the velocity and p is the pressure.

If there is a non-zero flow of the fluid through the boundary, there are several sets of boundary conditions on the parts of the boundary where the fluid enters the flow domain (the inlet) and leaves it (the outlet) which lead to mathematically correct initial-boundary-value problems (for references, see Antontsev et al. , 1990; Morgulis & Yudovich , 2002). One set of boundary conditions is where the normal and tangent components of the velocity is given at the inlet, but only the normal component of the velocity is prescribed at the outlet. It has been shown by Kazhikhov (see Chapter 4 in Antontsev et al. , 1990) that an initial-boundary-value problem for the Euler equations with these boundary conditions is a well-posed problem. In what follows we always consider the same boundary conditions at the inlet: both components of the velocity are prescribed. We shall refer to these conditions, supplemented with a condition for the normal component of velocity at the outlet, as the *normal velocity conditions*.

Here our focus is on a different set of boundary conditions: at the flow inlet, we have the same conditions as before (both the normal and tangent components of the velocity are prescribed), but at the outlet, the pressure is given instead of the normal velocity. The Euler equations with these boundary

conditions has been studied by Kazhikhov & Ragulin (1983), who have shown that the corresponding mathematical problem is well-posed. We shall call these conditions the *pressure conditions*.

Thus, our boundary conditions are

$$u|_{r=1} = 1, \quad v|_{r=1} = \gamma_1, \quad p|_{r=a} = p_0, \quad (2.4)$$

for the diverging flow ($\beta = 1$) and

$$u|_{r=a} = -\frac{1}{a}, \quad v|_{r=a} = \frac{\gamma_2}{a}, \quad p|_{r=1} = p_0, \quad (2.5)$$

for the converging flow ($\beta = -1$). Here $a = r_2/r_1$, p_0 and $\gamma_{1,2}$ are constants (p_0 is the dimensionless pressure at the outlet and $\gamma_{1,2}$ are the ratios of the azimuthal velocity to the radial velocity at the inner and outer cylinders, respectively)¹.

Equations (2.1)–(2.3) with boundary conditions, given by either (2.4) or (2.5), have the following simple rotationally-symmetric solutions:

$$u(r, \theta) = \frac{\beta}{r}, \quad v(r, \theta) = \begin{cases} \gamma_1/r, & \text{if } \beta = 1 \\ \gamma_2/r, & \text{if } \beta = -1 \end{cases} \quad (2.6)$$

with the pressure given by

$$p = p_0 - \frac{1 + \gamma_1^2}{2} \left(\frac{1}{r^2} - \frac{1}{a^2} \right) \quad (2.7)$$

for the diverging flow ($\beta = 1$) and by

$$p = p_0 + \frac{1 + \gamma_2^2}{2} \left(1 - \frac{1}{r^2} \right) \quad (2.8)$$

for the converging flow ($\beta = -1$). In the next section we investigate the stability of these steady flows.

2.2 Inviscid stability analysis

We consider a small perturbation $(\tilde{u}, \tilde{v}, \tilde{p})$ in the form of the normal mode

$$\{\tilde{u}, \tilde{v}, \tilde{p}\} = \text{Re} \left[\{\hat{u}(r), \hat{v}(r), \hat{p}(r)\} e^{\sigma t + i n \theta} \right] \quad (2.9)$$

where $n \in \mathbb{Z}$. This leads to the linearised equations:

$$\left(\sigma + \frac{i n \gamma_\alpha}{r^2} + \frac{\beta}{r} \partial_r \right) \hat{u} - \frac{\beta}{r^2} \hat{u} - \frac{2 \gamma_\alpha}{r^2} \hat{v} = -\hat{p}_r, \quad (2.10)$$

$$\left(\sigma + \frac{i n \gamma_\alpha}{r^2} + \frac{\beta}{r} \partial_r \right) \hat{v} + \frac{\beta}{r^2} \hat{v} = -\frac{i n}{r} \hat{p}, \quad (2.11)$$

$$\frac{1}{r} (r \hat{u})_r + \frac{i n}{r} \hat{v} = 0, \quad (2.12)$$

where $\gamma_\alpha = \gamma_1$ if $\beta = 1$ and $\gamma_\alpha = \gamma_2$ if $\beta = -1$, and the two sets of boundary conditions

$$\hat{u}(1) = 0, \quad \hat{v}(1) = 0, \quad \hat{p}(a) = 0 \quad (2.13)$$

for the diverging flow ($\beta = 1$) and

$$\hat{u}(a) = 0, \quad \hat{v}(a) = 0, \quad \hat{p}(1) = 0 \quad (2.14)$$

¹In general, one can consider non-constant $\gamma_{1,2}$ and p_0 , i.e. given functions $\gamma_{1,2}(\theta, t)$ and $p_0(\theta, t)$, consistent with the restriction that $u|_{r=a} > 0$ if $\beta = 1$ and $u|_{r=1} < 0$ if $\beta = -1$ for all θ and t .

for the converging flow ($\beta = -1$). Equations (2.10)–(2.12) with either set of boundary conditions represent an eigenvalue problem for σ .

First we note that both eigenvalue problems have no nontrivial solution for $n = 0$. Indeed, Eq. (2.12) for $n = 0$ and the boundary conditions for \hat{u} imply that $\hat{u} = 0$. Equation (2.11) yields $\hat{v} = C r^{-1} e^{-\sigma r^2/2\beta}$ where C is an arbitrary constant. Substitution of this into the boundary condition $\hat{v}(1) = 0$ for $\beta = 1$ or $\hat{v}(a) = 0$ for $\beta = -1$ leads to the conclusion that $C = 0$. So, from now on we focus on eigenvalue problems with $n \neq 0$.

It is convenient to introduce the stream function $\hat{\psi}(r)$ such that

$$\hat{u} = \frac{in}{r} \hat{\psi}(r), \quad \hat{v} = -\hat{\psi}'(r).$$

Eliminating the pressure from Eqs. (2.10) and (2.11), we obtain

$$\left(\sigma + \frac{in\gamma_\alpha}{r^2} + \frac{\beta}{r} \partial_r \right) L\hat{\psi} = 0, \quad (2.15)$$

where

$$L\hat{\psi} = \hat{\psi}'' + \frac{1}{r} \hat{\psi}' - \frac{n^2}{r^2} \hat{\psi}. \quad (2.16)$$

It follows from (2.15) that

$$L\hat{\psi} = C e^{-\beta g_\alpha(r)} \quad (2.17)$$

where C is a constant and $g_\alpha(r) = \sigma r^2/2 + in\gamma_\alpha \ln r$ for $\alpha = 1, 2$. The general solution of (2.17) can be written as

$$\hat{\psi} = \frac{C_1}{r^n} + C_2 r^n + \frac{C}{2n} \int_1^r \left(r^n s^{-n+1} - r^{-n} s^{n+1} \right) e^{-\beta g_\alpha(s)} ds \quad (2.18)$$

where C , C_1 and C_2 are arbitrary constants.

2.2.1 Diverging flow ($\beta = 1$)

Now consider the diverging flow ($\beta = 1$). In terms of $\hat{\psi}(r)$, the first two boundary conditions (2.13) take the form

$$\hat{\psi}(1) = 0, \quad \hat{\psi}'(1) = 0.$$

Substitution of the general solution, given by (2.18), into these conditions yields $C_1 = C_2 = 0$, so that Eq. (2.18) simplifies to

$$\hat{\psi} = \frac{C}{2n} \int_1^r \left(r^n s^{-n+1} - r^{-n} s^{n+1} \right) e^{-g_1(s)} ds \quad (2.19)$$

To satisfy the last of the boundary conditions (2.13), we employ Eq. (2.11). As a result, we obtain

$$\left(\sigma + \frac{in\gamma_1}{r^2} + \frac{1}{r} \partial_r \right) (r \partial_r \hat{\psi}) \Big|_{r=a} = 0. \quad (2.20)$$

Substitution of (2.19) into (2.20) yields the dispersion relation for σ :

$$D(\sigma, n, a, \gamma_1) \equiv \left(a^2 \sigma + in\gamma_1 + n \right) a^{n-3} I_1 + \left(a^2 \sigma + in\gamma_1 - n \right) a^{-(n+3)} I_2 + \frac{2}{a} e^{-g_1(a)} = 0 \quad (2.21)$$

where

$$I_1 = \int_1^a r^{-n+1} e^{-g_1(r)} dr, \quad I_2 = \int_1^a r^{n+1} e^{-g_1(r)} dr. \quad (2.22)$$

Evidently, the dispersion relation has the following properties

$$\overline{D(\sigma, n, a, \gamma_1)} = D(\overline{\sigma}, -n, a, \gamma_1), \quad D(\sigma, -n, a, -\gamma_1) = D(\sigma, n, a, \gamma_1).$$

(Here ‘bar’ denotes complex conjugation.) These properties imply that we need to consider only positive n and γ_1 .

Numerical evaluation of the dispersion relation shows that there are no eigenvalues with positive real parts if $\gamma_1 = 0$. If γ_1 increases from 0, the roots of Eq. (2.21) move on the complex plane and, at some critical value, $\gamma_1 = \gamma_{1cr}$, one of the eigenvalues crosses the imaginary axis, so that for $\gamma_1 > \gamma_{1cr}$ there is an eigenvalue with positive real part, and hence, the flow is unstable.

Numerical calculations produced the stability diagram presented in Fig. 1. It shows neutral curves on the (a, γ_1) plane for normal modes with $n = 1, \dots, 6$. The instability region for each mode is above the corresponding curve. Solid curves represent neutral curves for the pressure conditions. Dashed curves show the results of Ilin & Morgulis (2013) for the normal velocity condition. For all curves in Fig. 1, $\text{Im}(\sigma) \neq 0$. This means that the instability is oscillatory, and neutral modes are periodic azimuthal waves.

Although the neutral curves in both problems look qualitatively similar, there are two interesting differences, namely:

- (i) For each azimuthal mode, the curve for the problem considered in the present paper is below the one corresponding to the normal velocity condition, which means that the same flow is more unstable if the pressure condition is used, and the gap between each pair of curves corresponding to the same n is larger for smaller a .
- (ii) For the problem with the normal velocity condition, the critical value of γ_1 is a monotone decreasing function of a , for all azimuthal modes. However, in the case of the pressure condition, the neutral curves for modes with higher azimuthal wave numbers (for $n = 3, \dots, 6$) have a local minimum, and the minimum is attained at smaller values of a for higher n .

We should mention here a recent paper by Guadagni et al (2020). Motivated by an application to a flow in a radial vaneless diffuser, the authors studied the stability of the diverging flow given by Eqs. (2.6) and (2.7). Although the paper contains several typos/errors (most notably, in the dispersion relation), the neutral curves presented there seem to agree with the curves in Fig. 1.

Remark 1 (on the limit of weak radial flow). It can be shown that, in the limit $\gamma_1 \rightarrow \infty$,

$$\sigma = -in\gamma_1 + \gamma_1^{1/2} \left(\lambda + O(\gamma_1^{-1/2}) \right).$$

where λ is a root of the equation

$$\int_0^\infty e^{-\lambda x + inx^2} dx = 0.$$

The corresponding eigenfunction is given by

$$\hat{\phi}(r) = \left[F(\xi) - \frac{F(0)r^n}{1 + a^{2n}} \left(1 + a^{2n}/r^{2n} \right) \right]$$

where

$$F(\xi) = \int_\xi^\infty (x - \xi) e^{-\lambda x + inx^2} dx, \quad \xi = \gamma_1^{1/2}(r - 1).$$

The derivation of this approximation simply repeats the arguments laid down in Ilin & Morgulis (2013) (see also Kerswell, 2015) for the case of the normal velocity conditions.

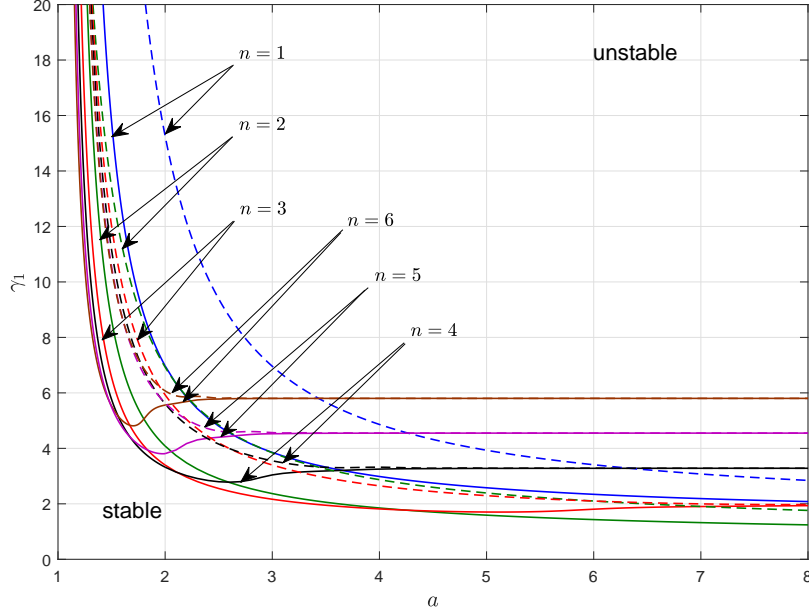


Figure 1: Diverging flow: solid curves represent neutral curves for azimuthal modes with $n = 1, \dots, 6$; dashed curves show neutral curves for the normal velocity condition, taken from Ilin & Morgulis (2013).

It turns out that the leading-order approximations to σ are the same for both types of boundary conditions. This suggests that, for $\gamma_1 \gg 1$, the instability in both problems has the same mechanism. This, however, does not mean that the change in the boundary condition at the outlet has little effect for all values of γ_1 . Indeed, the difference in the stability properties of the same flow in these two problems is considerable, as one can see in Fig. 1.

2.2.2 Converging flow ($\beta = -1$)

For the converging flow, similar calculations yield the following dispersion relation:

$$\tilde{D}(\sigma, n, a, \gamma_2) \equiv (\sigma + i n \gamma_2 - n) \tilde{I}_1 + (\sigma + i n \gamma_2 + n) \tilde{I}_2 + 2 e^{g_2(1)} = 0 \quad (2.23)$$

where

$$\tilde{I}_1 = \int_1^a r^{-n+1} e^{g_2(r)} dr, \quad \tilde{I}_2 = \int_1^a r^{n+1} e^{g_2(r)} dr. \quad (2.24)$$

Evidently, the dispersion relation has the same properties as those for the diverging flow:

$$\overline{\tilde{D}(\sigma, n, a, \gamma_2)} = \tilde{D}(\overline{\sigma}, -n, a, \gamma_2), \quad \tilde{D}(\sigma, -n, a, -\gamma_2) = \tilde{D}(\sigma, n, a, \gamma_2).$$

Again, these imply that we need to consider only positive n and γ_2 .

The neutral curves on the (a, γ_2) plane for modes with $n = 1, \dots, 6$ are shown in Fig. 2. The instability region for each mode is above the corresponding curve. Again, the solid curves represent neutral curves for the pressure conditions, and the dashed curves are curves for the normal velocity conditions computed in Ilin & Morgulis (2013). Qualitatively, the only difference between Figs. 1 and 2 is that every neutral curve in the latter has a local minimum. Conclusions (i) and (ii) and the remark on the limit of weak radial flow made for the diverging flows are also true for the converging flows.

In the next section, we shall discuss the effects of viscosity.

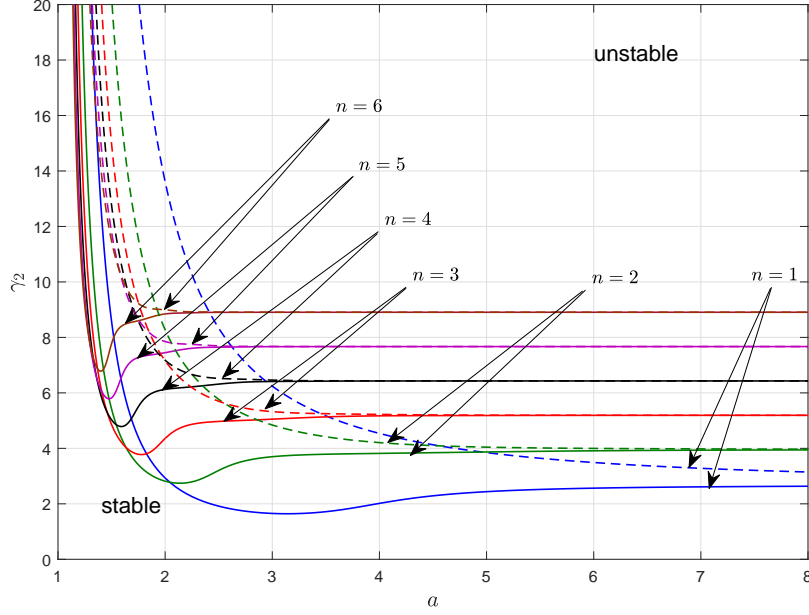


Figure 2: Converging flow: solid curves represent neutral curves for azimuthal modes with $n = 1, \dots, 6$; dashed curves show the results for the normal velocity conditions.

3 Effects of viscosity

Here we consider two-dimensional viscous flows in an annulus with the pressure-stress and pressure-no-slip conditions. The two-dimensional Navier-Stokes equations, written using the same non-dimensional variables as those in section 2.1, have the form

$$u_t + uu_r + \frac{v}{r}u_\theta - \frac{v^2}{r} = -p_r + \frac{1}{R} \left(\nabla^2 u - \frac{u}{r^2} - \frac{2}{r^2}v_\theta \right), \quad (3.1)$$

$$v_t + uv_r + \frac{v}{r}v_\theta + \frac{uv}{r} = -\frac{1}{r}p_\theta + \frac{1}{R} \left(\nabla^2 v - \frac{v}{r^2} + \frac{2}{r^2}u_\theta \right), \quad (3.2)$$

$$\frac{1}{r}(ru)_r + \frac{1}{r}v_\theta = 0, \quad (3.3)$$

where $R = |Q|/\nu$ is the radial Reynolds number (ν is the kinematic viscosity of the fluid) and ∇^2 is the polar form of the Laplace operator:

$$\nabla^2 = \partial_r^2 + \frac{1}{r}\partial_r + \frac{1}{r^2}\partial_\theta^2.$$

Both components of the velocity are prescribed at the inlet:

$$u|_{r=1} = 1, \quad v|_{r=1} = \gamma_1 \quad (3.4)$$

for the diverging flow ($\beta = 1$) and

$$u|_{r=a} = -\frac{1}{a}, \quad v|_{r=a} = \frac{\gamma_2}{a} \quad (3.5)$$

for the converging flow ($\beta = -1$).

The boundary conditions at the outlet are as follows.

(i) *The pressure-stress conditions:* for the diverging flows, these are given by

$$\left(-p + \frac{2}{R}u_r\right)\Big|_{r=a} = -p_0, \quad (3.6)$$

$$\frac{1}{R}\left(\frac{1}{r}u_\theta + v_r - \frac{1}{r}v\right)\Big|_{r=a} = s_0, \quad (3.7)$$

and, for the converging flows, by

$$\left(-p + \frac{2}{R}u_r\right)\Big|_{r=1} = -p_0, \quad (3.8)$$

$$\frac{1}{R}\left(\frac{1}{r}u_\theta + v_r - \frac{1}{r}v\right)\Big|_{r=1} = s_0, \quad (3.9)$$

where p_0 and s_0 are constants. For the converging flow, the sign of s_0 in Eq. (3.9) is chosen so as to make this condition look similar to condition (3.7). This means that $(-s_0)$ (not s_0 as in Eq. (3.7)) is the external tangential force (per unit area).

(ii) *The pressure-no-slip conditions* are

$$\left(-p + \frac{2}{R}u_r\right)\Big|_{r=a} = -p_0, \quad v|_{r=a} = \frac{\gamma_2}{a} \quad (3.10)$$

for the diverging flow and

$$\left(-p + \frac{2}{R}u_r\right)\Big|_{r=1} = -p_0, \quad v|_{r=1} = \gamma_1 \quad (3.11)$$

for the converging flow. Here $\gamma_{1,2}$ are the same non-dimensional parameters as before.

In the limit $R \rightarrow \infty$ conditions (3.6)–(3.9) and (3.10), (3.11) reduce to the inviscid boundary conditions of section 2. This limit is not uniform as there is a viscous boundary layer at the outlet (but not at the inlet). This is similar to the case of the reference boundary conditions, for which it is known that in the limit of high Reynolds number the boundary layer is formed at the outflow part of the boundary (see, e.g., Temam & Wang, 2000; Yudovich, 2001; Ilin, 2008).

Remark 2 (on relevance of the pressure-no-slip and pressure-stress conditions to real flows). As was mentioned in section 1, both the reference boundary conditions and the conditions considered in this paper can be used to model flows bounded by porous walls if we assume that the flow in the porous walls is known. In a more realistic model, one needs to solve the Navier-Stokes equations in the free flow domain and match it with a solution for a flow in the porous medium of the walls (e.g. described by Darcy's law), using appropriate boundary conditions. There are numerous papers on boundary conditions on an interface between a free fluid and porous medium (see, e.g., Beavers & Joseph, 1967; Saffman, 1971; Haber & Mauri, 1983). There seems to be a consensus that the normal velocity and the normal stress must be continuous across the interface. As for the tangential velocity, either the no-slip condition (with the tangential velocity in the porous medium being zero) or the Beavers-Joseph condition (see Beavers & Joseph, 1967; Saffman, 1971) are used. In what follows, we assume that the porous medium is anisotropic, with its permeability in the tangential direction being much smaller than the permeability in the normal direction, so that the tangential velocity in the walls is very small and can be ignored. As a result, we have the no-slip condition for the free fluid velocity. There are still two more conditions on the interface (for the normal velocity and the normal stress). If we do not want to consider the flow in the porous medium and assume that it is known, one of these conditions should be discarded in order to obtain a solvable mathematical problem for the Navier-Stokes equations. The most common approach

(see Bahl , 1970; Min & Lueptow , 1994; Serre et al , 2008; Martinand et al , 2009; Gallet et al. , 2010; Fujita et al. , 1997; Kerswell , 2015; Martinand et al , 2017; Ilin & Morgulis , 2015, 2020) is to assume that the normal velocity in the porous medium is known and discard the condition for the normal stress. This results in the reference conditions. However, one can drop the normal velocity condition instead. The result will be the pressure-no-slip conditions. Note that sometimes it is desirable to keep the condition for normal stress because it is physically preferable to assume that the pressure (rather than the normal velocity) in the porous medium is known or simply because it is less restrictive. Indeed, suppose that we investigate the stability of purely azimuthal flow between rotating porous cylinders to perturbations which do not change the boundary data. Then, if we use the reference boundary conditions, the perturbation velocity will have to be zero at both cylinders and we end up with the stability problem for the classical Couette-Taylor flow between rotating impermeable cylinders, so that the fact that the cylinders are porous does not make any difference. However, if we prescribe the normal stress instead of the normal velocity, there will be perturbations with nonzero normal velocity at the porous cylinders, which is more reasonable from the physical viewpoint.

The pressure-stress condition can also be applicable to real flows. Consider, for example, a situation where the fluid leaves the flow domain to an ambient fluid which is at rest. In this case, it is natural to assume that the normal force at the outlet is a force due to a constant pressure in the ambient fluid and that the tangential force is zero. For example, these conditions can be used to model flows in vaneless diffusers of radial pumps (see, e.g., Guadagni et al , 2020).

3.1 Basic flow

Steady rotationally-symmetric flows whose stability we want to examine are given by

$$u = \frac{\beta}{r}, \quad v = V(r) = A r^{\beta R+1} + \frac{B}{r} \quad (3.12)$$

where constants A and B are different for different boundary conditions at the outlet. For both sets of boundary conditions, the pressure is given by

$$p = P(r) = p_0 - \frac{2R^{-1}}{a^2} - \frac{1}{2} \left(\frac{1}{r^2} - \frac{1}{a^2} \right) - \int_r^a \frac{V^2(s)}{s} ds$$

for the diverging flow ($\beta = 1$) and

$$p = P(r) = p_0 + 2R^{-1} + \frac{1}{2} \left(1 - \frac{1}{r^2} \right) + \int_1^r \frac{V^2(s)}{s} ds$$

for the converging flow ($\beta = -1$)

The pressure-stress conditions. Constants A and B are given by the following formulae:

$$A = \frac{(s_0 + 2\gamma_1 a^{-2} R^{-1}) a^{-R}}{1 + 2R^{-1} a^{-(2+R)}}, \quad B = \frac{\gamma_1 - s_0 a^{-R}}{1 + 2R^{-1} a^{-(2+R)}} \quad (3.13)$$

for the diverging flow ($\beta = 1$) and

$$A = -\frac{s_0 + 2\gamma_2 R^{-1}}{1 - 2R^{-1} a^{2-R}}, \quad B = \frac{\gamma_2 + s_0 a^{2-R}}{1 - 2R^{-1} a^{2-R}} \quad (3.14)$$

for the converging flow ($\beta = -1$). The steady solution formula for the converging flow ($\beta = -1$) is not defined for $R = 2$. In this case, the solution is given by

$$u = -\frac{1}{r}, \quad v = V(r) = \tilde{A} \frac{\ln r}{r} + \frac{\tilde{B}}{r} \quad (3.15)$$

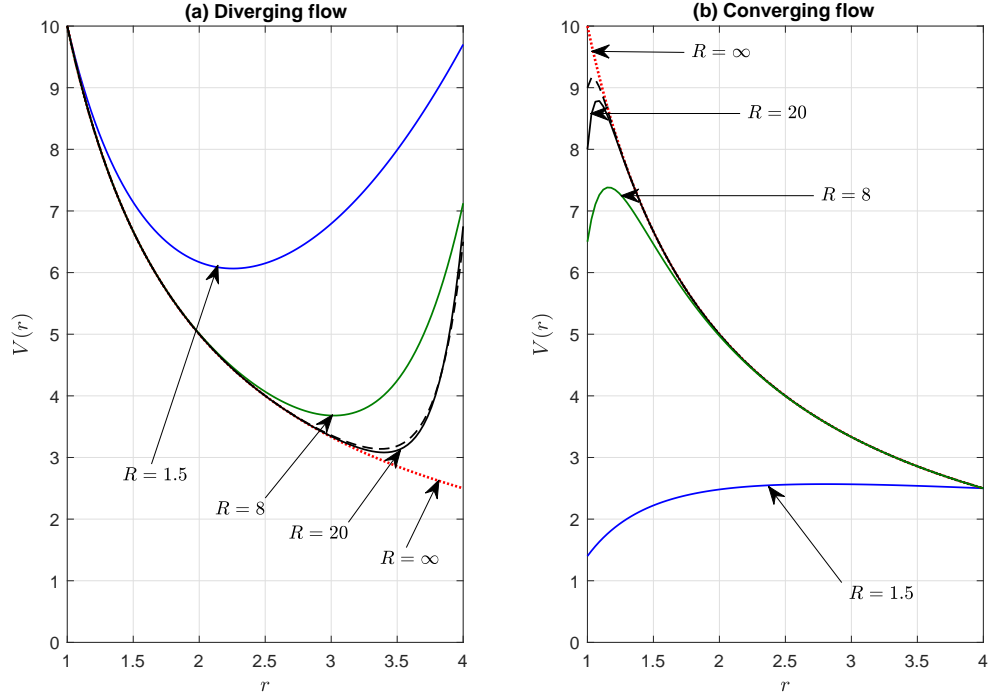


Figure 3: Typical velocity profiles for $a = 4$ and $R = 1.5, 8, 20$. (a) corresponds to the diverging flow ($\beta = 1$) with $\gamma_1 = 10$ and $s_0 = 1$, (b) corresponds to the converging flow ($\beta = -1$) with $\gamma_2 = 10$ and $s_0 = 1$. Dotted curves represent the inviscid velocity profiles. Dashed curves show $V(r)$ computed using the asymptotic formulae ($R \gg 1$) for $R = 20$.

where

$$\tilde{A} = \frac{2\gamma_2 + s_0}{1 + 2 \ln a}, \quad \tilde{B} = \frac{\gamma_2 - 2s_0 \ln a}{1 + 2 \ln a}.$$

The dependence of the steady flow (3.12)–(3.14) on R is non-trivial and, for $R \gg 1$, it has a boundary layer either at the outer cylinder (for the diverging flow) or at the inner one (for the converging flow).

It can be shown that, for $R \gg 1$, the azimuthal velocity profile is well approximated by the following asymptotic formula:

$$V(r) = \begin{cases} \gamma_1/r + s_0 a e^{-\eta} + O(R^{-1}) & \text{for } \beta = 1 \\ \gamma_2/r - s_0 e^{-\xi} + O(R^{-1}) & \text{for } \beta = -1 \end{cases}$$

where $\xi = R(r - 1)$ and $\eta = R(1 - r/a)$. Note that if $s_0 = 0$ (or if $s_0 \lesssim R^{-1}$ as $R \rightarrow \infty$), the above asymptotic formula is different:

$$V(r) = \begin{cases} \gamma_1/r + \frac{2\gamma_1}{a} e^{-\eta} R^{-1} + O(R^{-2}) & \text{for } \beta = 1 \\ \gamma_2/r - 2\gamma_2 e^{-\xi} R^{-1} + O(R^{-2}) & \text{for } \beta = -1 \end{cases}$$

which means that we have a weaker boundary layer.

Typical velocity profiles $V(r)$ for various R , as well as the corresponding asymptotic profiles given by the above formula, are shown in Fig. 3. Evidently, the asymptotic formulae produce good approximations to the exact profile even for $R = 20$.

The pressure-no-slip conditions. In this case, the azimuthal velocity profile is the same as the one

considered in Ilin & Morgulis (2015). Constants A and B can be written as

$$A = \frac{\gamma_2 - \gamma_1}{a^{\beta R+2} - 1}, \quad B = \frac{a^{\beta R+2} \gamma_1 - \gamma_2}{a^{\beta R+2} - 1}. \quad (3.16)$$

The steady solution depends on γ_1 , γ_2 and βR and is well defined for all $\beta R \neq -2$. For $\beta R = -2$, the solution is given by Eq. (3.15) with

$$\tilde{A} = \frac{\gamma_2 - \gamma_1}{\ln a}, \quad \tilde{B} = \gamma_1.$$

The asymptotic formula for $R \gg 1$ is

$$V(r) = \begin{cases} \gamma_1/r + ((\gamma_2 - \gamma_1)/a)e^{-\eta} + O(R^{-1}) & \text{if } \beta = 1 \\ \gamma_2/r - (\gamma_2 - \gamma_1)e^{-\xi} + O(R^{-1}) & \text{if } \beta = -1 \end{cases}$$

where the boundary layer variables ξ and η are the same as before: $\xi = R(r - 1)$ and $\eta = R(1 - r/a)$.

From now on, we study the stability of the above steady flows. The stability of steady flows in an annulus with the reference boundary conditions have been studied in detail in Ilin & Morgulis (2015). In what follows, all facts concerning the reference boundary conditions are taken from that paper.

3.2 Linear stability analysis

Consider a small perturbation in the form (2.9). The linearised equations have the form

$$\begin{aligned} \left(\sigma + \frac{inV_\beta}{r} + \frac{\beta}{r} \partial_r \right) \hat{u} - \frac{\beta}{r^2} \hat{u} - \frac{2V_\beta}{r} \hat{v} &= -\partial_r \hat{p} + \frac{1}{R} \left(L\hat{u} - \frac{\hat{u}}{r^2} - \frac{2in}{r^2} \hat{v} \right), \\ \left(\sigma + \frac{inV_\beta}{r} + \frac{\beta}{r} \partial_r \right) \hat{v} + \frac{\beta}{r^2} \hat{v} + \Omega_\beta(r) \hat{u} &= -\frac{in}{r} \hat{p} + \frac{1}{R} \left(L\hat{v} - \frac{\hat{v}}{r^2} + \frac{2in}{r^2} \hat{u} \right), \\ \partial_r (r\hat{u}) + in\hat{v} &= 0, \end{aligned} \quad (3.17)$$

In Eqs. (3.17), V_β with $\beta = \pm 1$ is the azimuthal velocity for the diverging ($\beta = 1$) and converging ($\beta = -1$) flows, and

$$L = \frac{d^2}{dr^2} + \frac{1}{r} \frac{d}{dr} - \frac{n^2}{r^2}, \quad \Omega_\beta(r) = V'_\beta(r) + \frac{V_\beta(r)}{r}.$$

At the inlet, the boundary conditions for Eqs. (3.17) are

$$\hat{u}(1) = 0, \quad \hat{v}(1) = 0 \quad (3.18)$$

for $\beta = 1$ and

$$\hat{u}(a) = 0, \quad \hat{v}(a) = 0 \quad (3.19)$$

for $\beta = -1$. At the outlet, the boundary conditions are either the pressure-stress conditions (that follow from Eqs. (3.6)–(3.9))

$$\hat{p}(a) = \frac{2}{R} \hat{u}'(a), \quad \frac{in}{a} \hat{u}(a) + \hat{v}'(a) - \frac{1}{a} \hat{v}(a) = 0 \quad (3.20)$$

for $\beta = 1$ and

$$\hat{p}(1) = \frac{2}{R} \hat{u}'(1), \quad in \hat{u}(1) + \hat{v}'(1) - \hat{v}(1) = 0 \quad (3.21)$$

for $\beta = -1$, or the pressure-no-slip conditions

$$\hat{p}(a) = \frac{2}{R} \hat{u}'(a), \quad \hat{v}(a) = 0 \quad (3.22)$$

for $\beta = 1$ and

$$\hat{p}(1) = \frac{2}{R} \hat{u}'(1), \quad \hat{v}(1) = 0 \quad (3.23)$$

for $\beta = -1$.

It can be shown that if we restrict our analysis to axisymmetric perturbations, then the basic steady flow (3.12) is asymptotically stable not only to small perturbations but also to perturbations of arbitrary amplitude. For the sake of completeness, the proof of this fact is given in Appendix A. In particular, it implies that the mode with $n = 0$ cannot be unstable for any value of the Reynolds number. So, we shall consider only the modes with $n \neq 0$.

In terms of the stream function $\hat{\psi}(r)$, the first two equations (3.17) are replaced by the vorticity equation

$$\left(\sigma + \frac{inV_\beta}{r} + \frac{\beta}{r} \partial_r \right) L\hat{\psi} - \frac{in}{r} \Omega'_\beta(r) \hat{\psi} = R^{-1} L^2 \hat{\psi}. \quad (3.24)$$

The inlet boundary conditions become

$$\hat{\psi}(1) = 0, \quad \hat{\psi}'(1) = 0 \quad \text{for } \beta = 1, \quad (3.25)$$

$$\hat{\psi}(a) = 0, \quad \hat{\psi}'(a) = 0 \quad \text{for } \beta = -1. \quad (3.26)$$

To find the pressure, we employ the second equation (3.17). As a result, we have

$$\hat{p} = \frac{ir}{nR} \left(L\hat{\psi}_r - \frac{\hat{\psi}_r}{r^2} + \frac{2n^2}{r^3} \hat{\psi} \right) - \frac{ir}{n} \left[\left(\sigma + \frac{inV_\beta}{r} + \frac{\beta}{r} \partial_r \right) \hat{\psi}_r + \frac{\beta}{r^2} \hat{\psi}_r - \frac{in}{r} \Omega_\beta \hat{\psi} \right].$$

So, the normal stress conditions at the outlet (the first equations in (3.20)–(3.23)) can be written as

$$\left[\frac{1}{R} \left(L\hat{\psi}_r - \frac{1+2n^2}{r^2} \hat{\psi}_r + \frac{4n^2}{r^3} \hat{\psi} \right) - \left(\sigma + \frac{inV_1}{r} + \frac{1}{r} \partial_r \right) \hat{\psi}_r - \frac{1}{r^2} \hat{\psi}_r + \frac{in}{r} \Omega_1 \hat{\psi} \right] \Big|_{r=a} = 0 \quad (3.27)$$

for $\beta = 1$ and

$$\left[\frac{1}{R} \left(L\hat{\psi}_r - \frac{1+2n^2}{r^2} \hat{\psi}_r + \frac{4n^2}{r^3} \hat{\psi} \right) - \left(\sigma + \frac{inV_{-1}}{r} - \frac{1}{r} \partial_r \right) \hat{\psi}_r + \frac{1}{r^2} \hat{\psi}_r + \frac{in}{r} \Omega_{-1} \hat{\psi} \right] \Big|_{r=1} = 0 \quad (3.28)$$

for $\beta = -1$. The tangent stress conditions at the outlet (the second equations in (3.20) and (3.21)) take the form

$$\hat{\psi}''(a) - \frac{1}{a} \hat{\psi}'(a) + \frac{n^2}{a^2} \hat{\psi}(a) = 0 \quad \text{for } \beta = 1, \quad (3.29)$$

$$\hat{\psi}''(1) - \hat{\psi}'(1) + n^2 \hat{\psi}(1) = 0 \quad \text{for } \beta = -1. \quad (3.30)$$

The no-slip conditions at the outlet (given by the second equations in (3.22) and (3.23)) become

$$\hat{\psi}'(a) = 0 \quad \text{for } \beta = 1 \quad \text{and} \quad \hat{\psi}'(1) = 0 \quad \text{for } \beta = -1. \quad (3.31)$$

Note that, in view of (3.31), conditions (3.27) and (3.28) simplify to

$$\left[\frac{1}{R} \left(\hat{\psi}_{rrr} + \frac{1}{r} \hat{\psi}_{rr} + \frac{4n^2}{r^3} \hat{\psi} \right) - \frac{1}{r} \hat{\psi}_{rr} + \frac{in}{r} \Omega_1 \hat{\psi} \right] \Big|_{r=a} = 0 \quad (3.32)$$

for $\beta = 1$ and

$$\left[\frac{1}{R} \left(\hat{\psi}_{rrr} + \frac{1}{r} \hat{\psi}_{rr} + \frac{4n^2}{r^3} \hat{\psi} \right) + \frac{1}{r} \hat{\psi}_{rr} + \frac{in}{r} \Omega_{-1} \hat{\psi} \right] \Big|_{r=1} = 0 \quad (3.33)$$

for $\beta = -1$.

Simply by looking at Eq. (3.24)–(3.31) and Eqs. (3.12)–(3.16), one can deduce the following. First, for a given β , an eigenvalue is a function of five parameters: $\sigma = \sigma(a, n, \gamma_1, \gamma_2, R)$ in the case of the pressure-no-slip conditions; $\sigma = \sigma(a, n, \gamma_\alpha, s_0, R)$, with $\alpha = 1$ for $\beta = 1$ and $\alpha = 2$ for $\beta = -1$, in the case of the pressure-stress conditions. Second, if $\sigma(a, n, \gamma_1, \gamma_2, R)$ (or $\sigma(a, n, \gamma_\alpha, s_0, R)$) is an eigenvalue, then so are $\bar{\sigma}(a, -n, \gamma_1, \gamma_2, R)$ (or $\bar{\sigma}(a, -n, \gamma_\alpha, s_0, R)$) and $\sigma(a, -n, -\gamma_1, -\gamma_2, R)$ (or $\sigma(a, -n, -\gamma_\alpha, -s_0, R)$). Here $\bar{\sigma}$ is the complex conjugate of σ . These properties imply that it suffices to consider only positive n and, also, a certain symmetry of the neutral curves (which will be used later).

For $R \gg 1$, an asymptotic theory of the eigenvalue problems with the pressure-stress or pressure-no-slip conditions can be developed along the same lines as in Ilin & Morgulis (2015). In particular, it can be shown that both problems reduce to the inviscid spectral problem of section 2.2. This is a non-trivial property because of the following two facts: (i) the basic viscous flow depends on the Reynolds number R , and (ii) a single inviscid steady flow represents a vanishing viscosity limit for continuous families of viscous steady flows (given by Eqs. (3.12)–(3.16)).

We shall not go into details of the asymptotic procedure here. Instead, we shall solve the viscous eigenvalue problems numerically.

3.3 Numerical results

The eigenvalue problems with the pressure-stress and pressure-no-slip conditions are solved numerically using the Galerkin method with polynomial basis functions based on Legendre polynomials. In the problem with the pressure-stress conditions, the basis functions are chosen to satisfy the boundary conditions at the inlet, given by Eqs. (3.25) or (3.26), and at the outlet by (3.29) or (3.30). So, $\hat{\psi}$ is approximated by

$$\hat{\psi}(r) = \sum_{k=0}^N c_k \phi_k(x), \quad x = -1 + \frac{2}{a-1}(r-1),$$

with basis functions $\phi_k(x)$, given by

$$\phi_k(x) = \begin{cases} (1+x)^2(x+\alpha_k)P_k(x), & \text{for } \beta = 1 \\ (1-x)^2(x+\alpha_k)P_k(x), & \text{for } \beta = -1 \end{cases}$$

for $k = 0, \dots, N$, where $P_k(x)$ is the Legendre polynomial of degree k and α_k is a constant chosen so as to satisfy (3.29) or (3.30) (note that conditions (3.25) or (3.26) are automatically satisfied). The normal stress condition, given by Eqs. (3.27) or (3.28), is satisfied using the τ -method (see, e.g., Gottlieb & Orszag, 1977).

In the case of the pressure-no-slip conditions, the τ -method yields spurious eigenvalues because conditions (3.32) and (3.33) do not contain the spectral parameter σ . However, the same fact makes it possible to construct basis functions which satisfy all the boundary conditions. These basis functions have the form

$$\phi_k(x) = \begin{cases} (1+x)^2(x^2 + \alpha_k x + \beta_k)P_k(x), & \text{for } \beta = 1 \\ (1-x)^2(x^2 + \alpha_k x + \beta_k)P_k(x), & \text{for } \beta = -1 \end{cases}$$

where constants α_k and β_k are chosen to satisfy the conditions given by the first equation (3.31) and Eq. (3.32) if $\beta = 1$ and the second equation (3.31) and Eq. (3.33) if $\beta = -1$.

To verify the method, some of the computed eigenvalues were compared with eigenvalues obtained using the shooting method. A further verification was provided by checking the consistency of the results for high radial Reynolds numbers with the inviscid theory of section 2.

3.3.1 Problem with the pressure-stress conditions.

Diverging flow. Figures 4 and 5 show neutral curves on the (γ_1, R) plane for $a = 2$ and $a = 8$, respectively. The solid curves represent critical values of R as functions of γ_1 for modes with $n = 1, \dots, 5$ for the

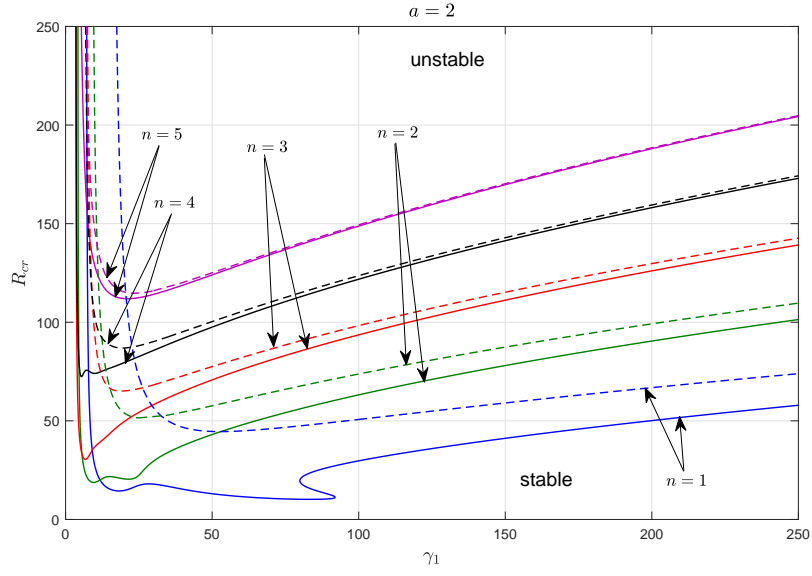


Figure 4: Diverging flow with the pressure-stress conditions: critical R versus γ_1 for $a = 2$ and $n = 1, \dots, 5$. Solid curves correspond to the pressure-stress conditions with $s_0 = 0$, dashed curves - to the reference conditions with $\gamma_2 = 0$.

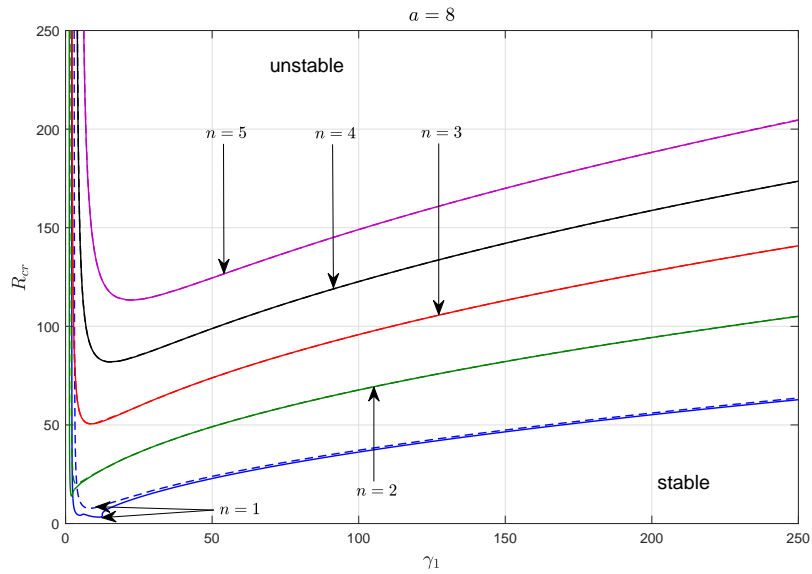


Figure 5: Diverging flow with the pressure-stress conditions: critical R versus γ_1 for $a = 8$ and $n = 1, \dots, 5$. Solid curves correspond to the pressure-stress boundary conditions with $s_0 = 0$, dashed curves - for the reference conditions with $\gamma_2 = 0$.

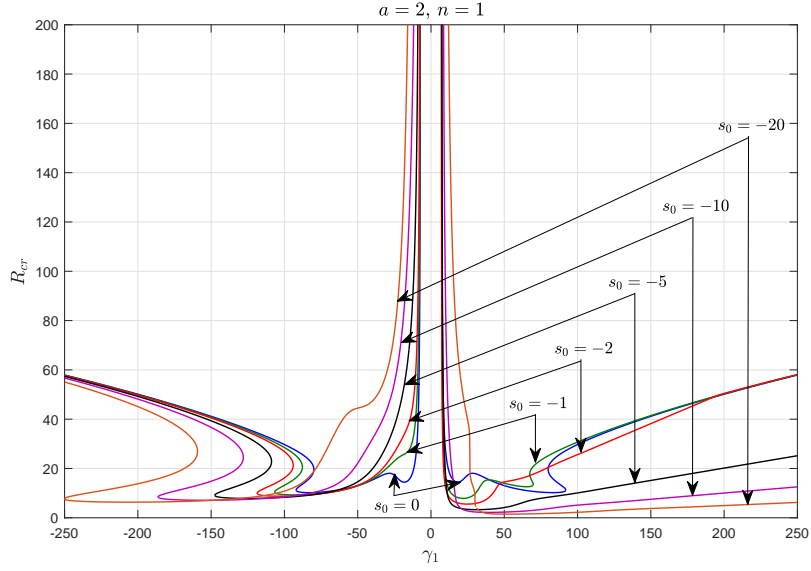


Figure 6: Diverging flow with the pressure-stress conditions: critical R versus γ_1 for $a = 2$, $n = 1$ and several values of s_0 .

pressure-stress conditions with $s_0 = 0$. The dashed curves are critical curves for the reference boundary conditions with $\gamma_2 = 0$, taken from Ilin & Morgulis (2015). All curves in Figs. 4 and 5 approach vertical asymptotes as γ_1 tends to $\gamma_1^*(a, n)$ from the right, where $\gamma_1^*(a, n)$ is the critical value of γ_1 for the inviscid mode with azimuthal number n . Numbers $\gamma_1^*(a, n)$ can be determined from the inviscid diagram shown in Fig. 1.

We note in passing that, in view of the symmetry properties of the eigenvalue problem, critical curves for negative γ_1 can be obtained by reflecting the curves in Figs. 4 and 5 about the vertical axis.

Figure 4 shows that the critical curves for $a = 2$ are below the corresponding curves for the problem with the reference boundary conditions, and the gap between the curves with the same azimuthal wave number n is larger for smaller n and decreases when n increases. The same is true for the critical curves for $a = 8$, but the effect is much weaker: one can see in Fig. 5 that the gap between the curves with $n = 1$ is much smaller than the corresponding gap for $a = 2$, and it becomes invisible for modes with $n > 1$. We can conclude that the pressure-stress boundary conditions make the flow more unstable, and this effect is stronger for smaller a . The latter is not surprising, as it is natural to expect that for wider annuli, the effect of the boundary conditions at the outlet is weaker.

Figure 6 shows critical curves for $a = 2$, $n = 1$ and several values of s_0 . While the curve for $s_0 = 0$ is symmetric relative to the vertical axis, the curves for $s_0 \neq 0$ are not symmetric. However, due to the symmetries of the eigenvalue problem mentioned earlier, the critical curves for the same a and n and for $s_0 = 0, 1, 2, 5, 10, 20$ can be obtained by reflecting the curves in Fig. 6 about the vertical axis $\gamma_1 = 0$. Note that most neutral curves in Fig. 6 have folds. This manifests itself especially clearly in the left half of the figure (where the directions of the tangent velocity at the inlet and tangent force at the outlet coincide). This means that for some fixed values of γ_1 , as the radial Reynolds number increases, the flow becomes unstable, then stable, then unstable again.

Converging flow. Figures 7 and 8 show critical curves on the (γ_2, R) plane for the converging flow ($\beta = -1$) for $a = 2$ and $a = 8$. The solid curves correspond to the pressure-stress conditions with $s_0 = 0$, and the dashed curves - to the reference boundary conditions with $\gamma_1 = 0$. Everything that has been said about the diverging flows can also be said about the neutral curves for the converging flows. The only

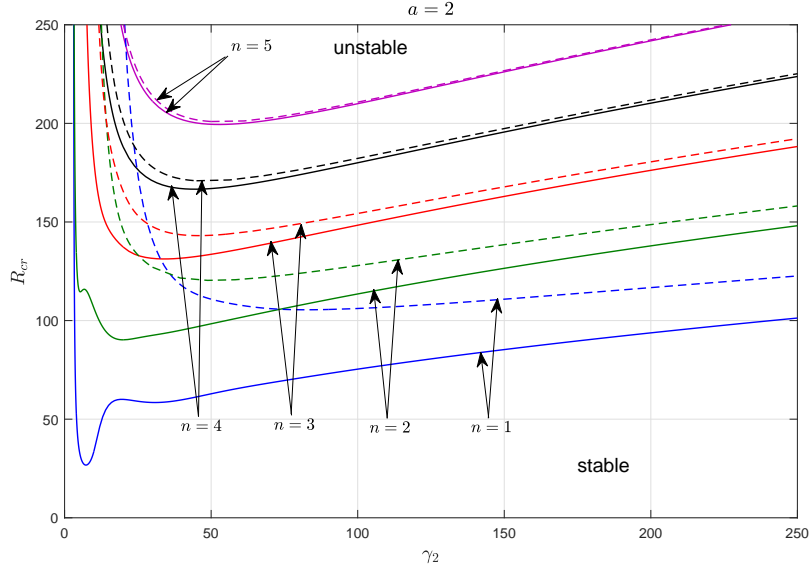


Figure 7: Converging flow with the pressure-stress conditions: critical R versus γ_2 for $a = 2$ and $n = 1, \dots, 5$. Solid curves correspond to the pressure-stress conditions with $s_0 = 0$, dashed curves - to the reference boundary conditions with $\gamma_1 = 0$.

difference is that the critical curves for the converging flows are above the corresponding curves for the diverging flows, i.e. the former are more stable than the latter, but we still have the result that the flows with the pressure-stress conditions are more unstable than those with the reference conditions.

Figure 9 shows critical curves for the converging flows for $a = 2$, $n = 1$ and several values of s_0 . The curve for $s_0 = 0$ is symmetric relative to the vertical axis, but the symmetry is lost for nonzero s_0 . Again, the critical curves for the same a and n and for $s_0 = 0, 1, 2, 5, 10, 20$ can be obtained by reflecting the curves in Fig. 9 about the vertical axis $\gamma_2 = 0$. Note the oscillatory behaviour of the curves near the axis $\gamma_2 = 0$, which implies that, for certain fixed values of R , the stability properties change a few times, when γ_2 increases. For very high R ($R \rightarrow \infty$), all critical curves approach the vertical asymptotes $\gamma_2 = \pm\gamma_2^*(a, n)$ irrespective of values of s_0 , where $\gamma_2^*(a, n)$ is the inviscid instability boundary on the (a, γ_2) plane, shown in Fig. 2.

There is an interesting feature in Fig. 9 (which is absent in Fig. 6), namely: the curves for $s_0 = -10$ and $s_0 = -20$ cross the vertical axis $\gamma_2 = 0$. More precisely, for the converging flows with sufficiently large (in magnitude) s_0 , there is a finite interval in R where the flow is unstable even for $\gamma_2 = 0$ (i.e. for purely radial flow at the inlet). For $s_0 = \pm 10$, this instability interval is $R \in (4.907, 61.417)$; for $s_0 = \pm 20$, it is $R \in (3.064, 243.605)$.

3.3.2 Problem with the pressure-no-slip conditions.

Diverging flow. The critical curves for the pressure-no-slip conditions (solid curves), as well as the curves for the reference conditions (dashed curves), are shown in Figs. 10(a) for $a = 2$ and 11(a) for $a = 8$. Figures 10(b) and 11(b) show the same curves for small R in more detail. Evidently, as $\gamma_1 \rightarrow \infty$, the neutral curves monotonically approach the horizontal line $R = 0$, which suggests that in the limit $\gamma_1 \rightarrow \infty$ (equivalently, in the limit of a weak radial flow), the basic flow is unstable for all $R > 0$. This behaviour is very different from both the case of the pressure-stress conditions and the case of the reference conditions, for which the critical Reynolds number grows linearly with γ_1 for $\gamma_1 \gg 1$.

The critical curves for $a = 2$, $n = 1$ and several values of γ_2 are shown in Fig. 12. Again, the critical

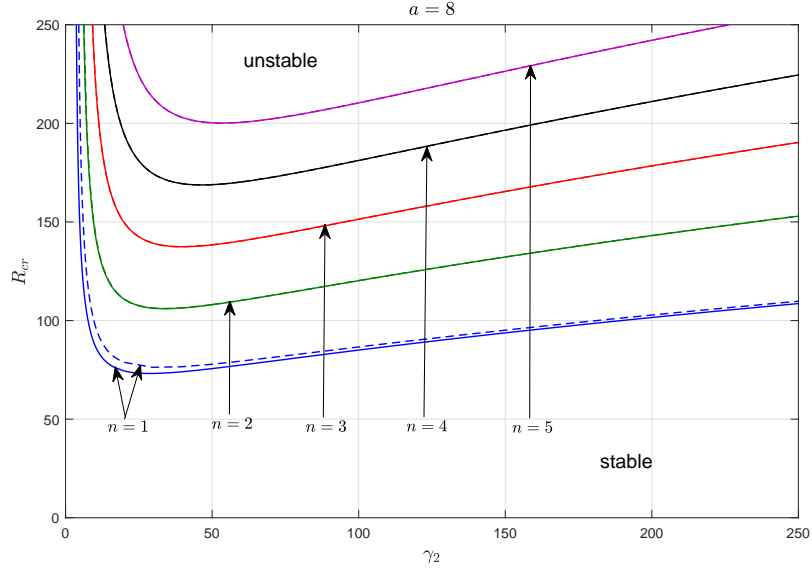


Figure 8: Converging flow with the pressure-stress conditions: critical R versus γ_2 for $a = 8$ and $n = 1, \dots, 5$. Solid curves correspond to the pressure-stress boundary conditions with $s_0 = 0$; dashed curves - to the reference boundary conditions with $\gamma_1 = 0$.

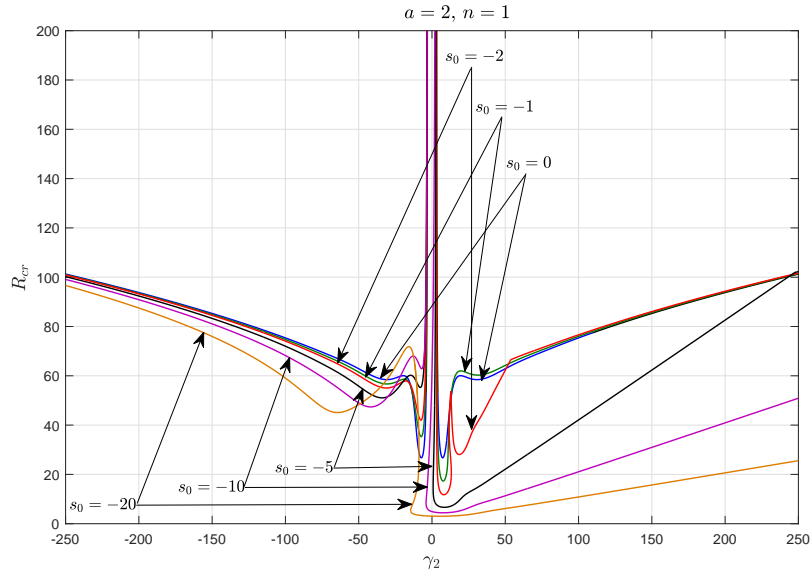


Figure 9: Converging flow with the pressure-stress conditions: critical R versus γ_2 for $a = 2$, $n = 1$ and several values of s_0 .

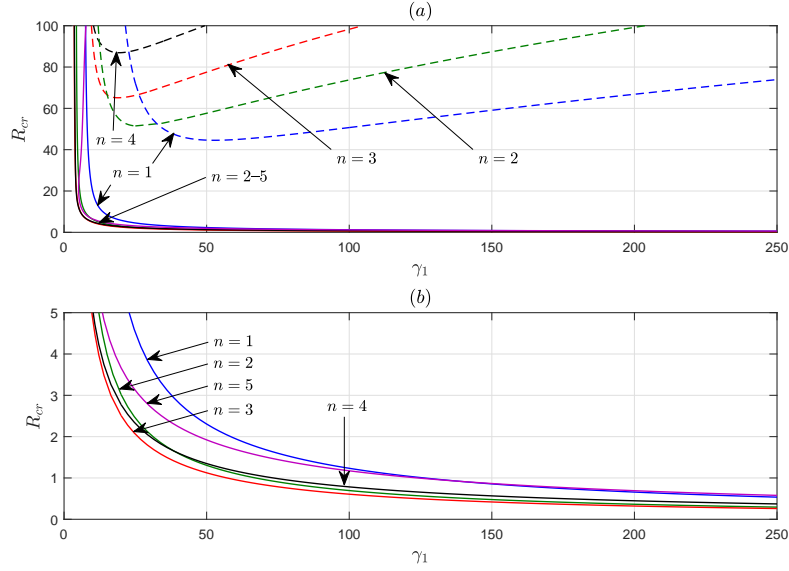


Figure 10: Diverging flow with the pressure-no-slip conditions: critical R versus γ_1 for $a = 2$, $\gamma_2 = 0$ and $n = 1, \dots, 5$; (a) solid curves correspond to the pressure-no-slip conditions, dashed curves - to the reference boundary conditions; (b) shows a magnified lower part of (a).

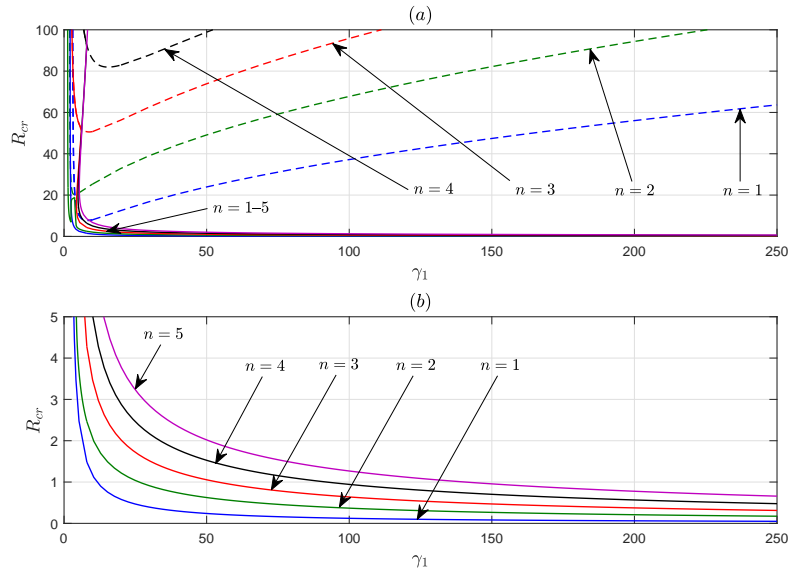


Figure 11: Diverging flow with the pressure-no-slip conditions: critical R versus γ_1 for $a = 8$, $\gamma_2 = 0$ and $n = 1, \dots, 5$; (a) solid curves correspond to the pressure-no-slip conditions, dashed curves - to the reference boundary conditions; (b) shows a magnified lower part of (a).

curves for the same a and n and for $\gamma_2 = 0, 20, 40, 60$ can be obtained by reflecting the curves in Fig. 12 about the vertical axis $\gamma_1 = 0$. Note that, for sufficiently large $|\gamma_1|$, the critical curves for all values of γ_2 approach the axis $R = 0$. So, this effect appears to be independent of γ_2 . Note also that the dependence of the critical curves on γ_2 (i.e. on what is happening at the outlet) is relatively weak in comparison with the case of the pressure-stress conditions (Fig. 6).

It turns out that it is possible to construct an asymptotic approximation of the eigenvalue problem for large γ_1 . This is done in Appendix B, where it is shown that, at leading order, the critical values of R are given by

$$R_{cr} = \frac{Re_{cr}(a, n)}{\gamma_1} + O(\gamma_1^{-1}) \quad (3.34)$$

where $Re_{cr}(a, n)$ is a certain critical value of the azimuthal Reynolds number, defined as

$$Re = \gamma_1 R = \frac{V_1^* r_1}{\nu}. \quad (3.35)$$

Here V_1^* is the azimuthal velocity in the basic flow at the inner cylinder. The leading-order approximations computed using Eq. (3.34), as well as the critical curves obtained by solving the original eigenvalue problem, are shown as dashed and solid curves, respectively, in Fig. 13. One can see that the dashed curves approach the solid curves as γ_1 increases, which indicates that the asymptotic formula (3.34), obtained in Appendix B, works. Note also that Re_{cr} depends only on a and n and does not depend on γ_2 , i.e. on the azimuthal velocity at the outlet (of course, higher-order approximations will depend on γ_2). This means that, at leading order, the asymptotic behaviour of the critical curves for $\gamma_2 \neq 0$ is the same as that for $\gamma_2 = 0$. This explains our earlier observation that the critical curves for all values of γ_2 approach the axis $R = 0$ as $\gamma_1 \rightarrow \infty$.

The fact that the flow becomes unstable at an arbitrarily small radial Reynolds number provided that $|\gamma_1|$ is sufficiently large is quite unexpected because (in contrast with the case of the pressure-stress conditions) the basic flow is exactly the same as the one studied in Ilin & Morgulis (2015). The only difference is that here the normal velocity condition at the outlet is replaced by the normal stress condition. So, we can conclude that the normal stress condition drastically destabilizes the same viscous flow.

The asymptotic analysis of Appendix B has an interesting byproduct, namely: it turns out that the Couette-Taylor flow between rotating cylinders (with a rotating impermeable inner cylinder and a non-rotating permeable outer cylinder) is linearly unstable to two dimensional perturbations provided that the normal stress condition is imposed at the outer cylinder. This is in contrast with the well-known fact that the classical Couette-Taylor flow (with the normal velocity condition at the outer cylinder) is stable to two-dimensional perturbations. The instability of the flow studied in the present paper at very low radial Reynolds numbers is a direct consequence to this fact.

Converging flow. Critical curves for the converging flows with the pressure-no-slip conditions for $\gamma_1 = 0$ and $a = 2$ are shown in Fig. 14. Curves in the top half of the picture for $n = 1, \dots, 5$ are very similar to the critical curves for the problem with the reference conditions. These curves are associated with the inviscid instability of section 2 and approach the vertical asymptotes $\gamma_2 = \pm\gamma_2^*(a, n)$, where $\gamma_2^*(a, n)$ is the inviscid instability boundary on the (a, γ_2) plane, shown in Fig. 2. For each azimuthal mode with $n = 4, \dots, 7$, there are another two disjoint regions where the corresponding modes are unstable. This is also true for the mode with $n = 3$ but only one of the two regions is visible, as the other is outside the range of γ_2 in Fig. 2. For higher n , these two regions merge in to a single one (e.g. the curves for $n = 8$ and 9).

The instability regions that are in the right half of the figure, but not too close to the horizontal axis $R = 0$ are qualitatively similar to those discussed in Ilin & Morgulis (2013) and associated with the instability of the boundary layer at the outlet (which reduces to the instability of the asymptotic suction profile for $R \gg 1$). The instability regions that lie near the horizontal axis represent a new instability. Figure 15 shows that the lower boundary of these approaches $R = 0$ as $\gamma_2 \rightarrow \infty$. Asymptotic behaviour

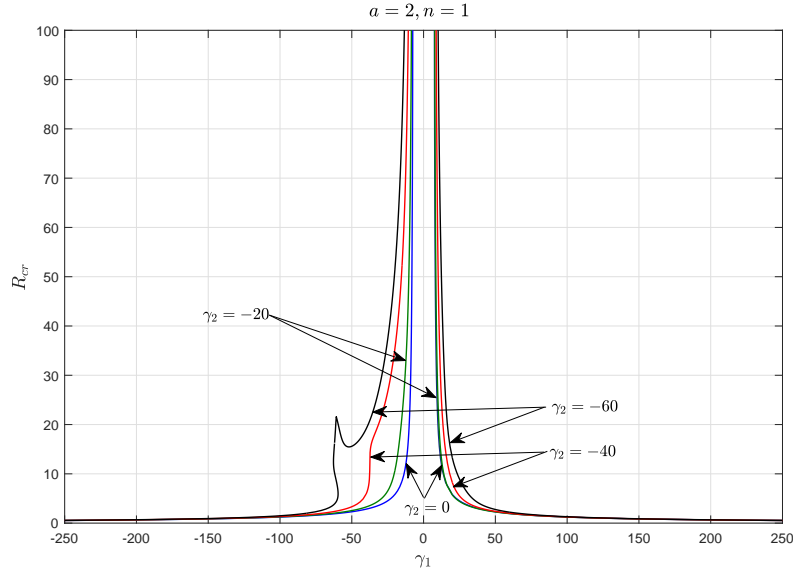


Figure 12: Diverging flow with the pressure-no-slip conditions: critical R versus γ_1 for $a = 2$, $n = 1$ and $\gamma_2 = 0, -20, -40, -60$.

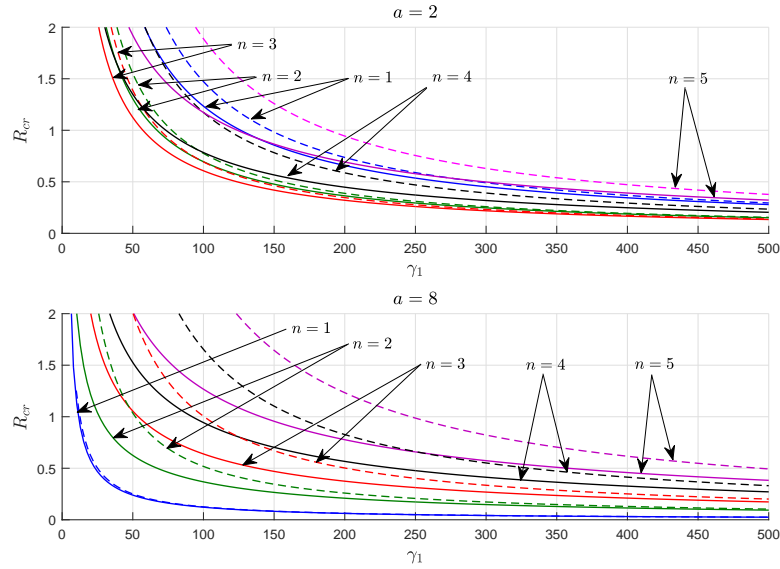


Figure 13: Diverging flow with the pressure-no-slip conditions: critical R versus γ_1 for large γ_1 for $a = 2$ (upper plot) and $a = 8$ (lower plot). Dashed curves show the leading-order asymptotic values of R_{cr} for $\gamma_1 \gg 1$.

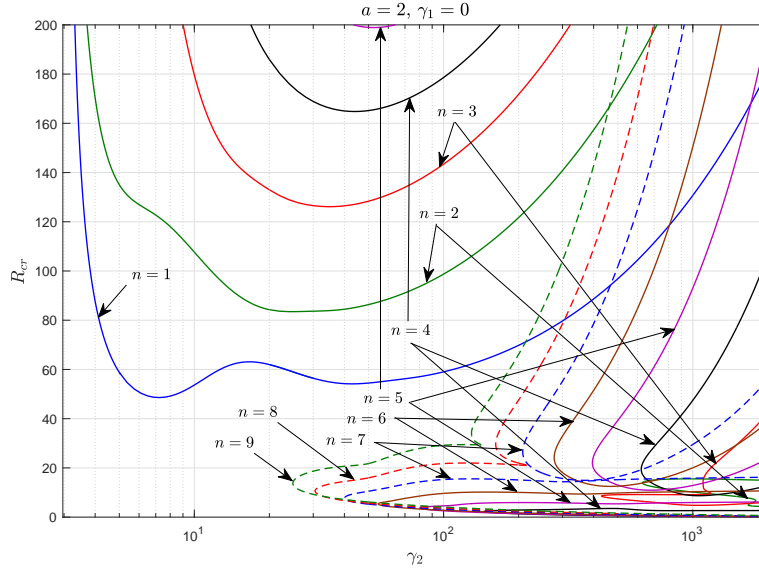


Figure 14: Converging flow with the pressure-no-slip conditions: critical R versus γ_2 for $a = 2$ and $\gamma_1 = 0$.

of these curves for $\gamma_2 \gg 1$ can be analysed in exactly the same manner as it was done for the diverging flows. It is shown in Appendix B that, at leading order, the critical values of R are given by

$$R_{cr} = \frac{\tilde{R}_{cr}(a, n)}{\gamma_2} + O\left(\gamma_2^{-1}\right) \quad (3.36)$$

where $\tilde{R}_{cr}(a, n)$ is a critical value of the azimuthal Reynolds number, defined as $\tilde{R}e = \gamma_2 R = V_2^* r_1 / \nu$ where V_2^* is the azimuthal velocity in the basic flow at the outer cylinder. The leading-order approximations given by Eq. (3.36) and the critical curves obtained by solving the original eigenvalue problem are shown as dashed and solid curves, respectively, in Fig. 15. Evidently, the dashed curves approach the solid curves as γ_2 increases, confirming that the asymptotic formula (3.36) is correct. Again, a byproduct of the asymptotic analysis is that the classical Couette-Taylor flow with a rotating impermeable outer cylinder and a non-rotating porous inner cylinder is unstable to two-dimensional perturbations if the normal stress condition is imposed at the inner cylinder. This is even more surprising than the analogous result for the diverging flow because it is well known that the classical Couette-Taylor flow is stable even to three-dimensional perturbations when the inner cylinder is non-rotating (see, e.g., Andereck et al , 1986; Chossat & Iooss , 1994).

Figure 16 shows critical curves for $a = 2$, $n = 1$ and $\gamma_1 = 0, -10, -20, -30$. As before, the critical curves for the same a and n and for $\gamma_1 = 0, 10, 20, 30$ can be obtained by reflecting the curves in Fig. 16 about the vertical axis $\gamma_2 = 0$. The same feature as in Fig. 9 for the pressure-stress conditions appears here: the curves for $\gamma_1 = -10, -20$ and -30 cross the vertical axis $\gamma_2 = 0$. For the converging flows with sufficiently large $|\gamma_1|$, there is a finite interval in R where the flow is unstable even for $\gamma_2 = 0$ (i.e. for purely radial flow at the inlet). For $\gamma_1 = \pm 10$, the flow is unstable if $R \in (10.38, 14.904)$; for $\gamma_1 = \pm 20$, if $R \in (3.693, 81.635)$; for $\gamma_1 = \pm 30$, if $R \in (2.588, 182.578)$. Again, for very high R ($R \rightarrow \infty$), all critical curves approach the same vertical asymptotes as before for all values of γ_1 .

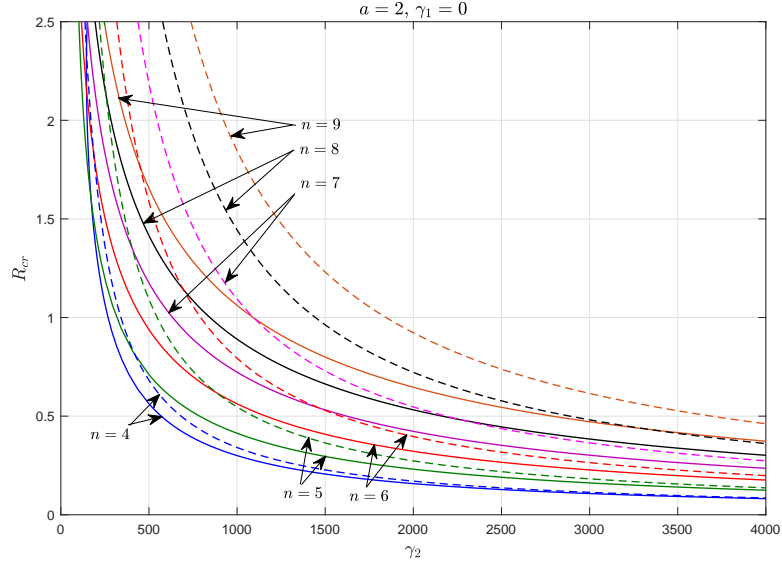


Figure 15: Converging flow with the pressure-no-slip conditions: critical R versus γ_2 for $\gamma_2 \gg 1$ for $a = 2$, $\gamma_1 = 0$ and $n = 4, \dots, 9$ (solid curves). Dashed curves show the leading-order asymptotic values of R_{cr} for $\gamma_2 \gg 1$.

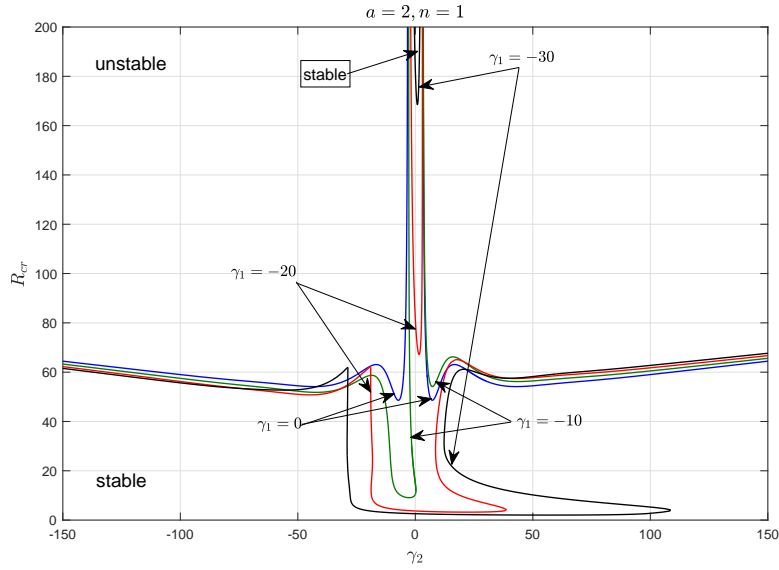


Figure 16: Converging flow with the tangent velocity conditions: critical R versus γ_2 for $a = 2$, $n = 1$ and $\gamma_1 = 0, -10, -20, -30$.

4 Discussion

We have shown that the instability of a simple steady inviscid flow found in Ilin & Morgulis (2013) also occurs if the normal velocity condition at the outlet is replaced by the pressure condition. Moreover, under the pressure condition, the flow is more unstable. We have also considered the stability of two families of steady viscous flows both of which reduce to the single inviscid flow with the pressure condition in the limit of high radial Reynolds numbers. For both families, all components of the velocity at the inlet, as well as the normal stress at the outlet were given. The only difference between them was in the second condition at the outlet where either the tangent stress or tangent velocity were prescribed. As one would expect, both families are instable due to the inviscid instability mechanism for sufficiently high R . However, it turned out that, for moderate and small radial Reynolds numbers, the stability properties (for both types of boundary conditions) may be very different from the results of Ilin & Morgulis (2015) obtained for the reference conditions. In most cases, the pressure-stress and pressure-no-slip conditions have a strong destabilising effect, because these conditions are less restrictive than the reference conditions (they allow perturbations with nonzero radial velocity at the outlet). In particular, in the problem with the pressure-no-slip conditions, both the diverging and converging flows turned out to be unstable for arbitrarily small R , provided that the azimuthal velocity at the inlet is much higher than the radial velocity. In these cases, we have derived asymptotic formulae for critical radial Reynolds number which agree with numerical calculations.

As a byproduct of these asymptotic formulae, we have found that two particular cases of the classical Couette-Taylor flow, where one, *impermeable* cylinder is rotating and the other, *permeable cylinder* is stationary, are unstable to two-dimensional perturbations provided that the normal stress condition (instead of the normal velocity condition) at the permeable cylinder is imposed. This is in contrast with the well-known fact that the Couette-Taylor flow is stable to two-dimensional perturbations. Moreover, in the case where the inner cylinder is non-rotating, the classical Couette-Taylor flow is stable even to three-dimensional perturbations (see, e.g., Andereck et al , 1986; Chossat & Iooss , 1994). The reason for this instability is that the normal stress condition at a porous wall allows nonzero flow into and out of the porous wall. In Fig. 17, typical contour plots of the stream function of neutral perturbations for both cases of the Couette-Taylor flow are shown. Evidently, for these neutral modes the normal velocity at the permeable cylinder is nonzero. Such modes are absent in the case of the reference boundary conditions.

Another interesting result, which is valid for both types of boundary conditions is that there are flow regimes where the converging flows are unstable even if the azimuthal velocity at the inlet is zero as one can see in Figs. 9 and 16.

The main conclusion of this paper is that boundary conditions at the outlet which include the normal stress condition may completely change the stability of the flow. This is particularly apparent in the case of the pressure-no-slip conditions where the basic steady flow is exactly the same as the one considered in Ilin & Morgulis (2015), yet the change of one boundary condition at the outlet makes the flow much more unstable for small and moderate values of R .

It was shown in Ilin & Morgulis (2015) that, in addition to an inviscid instability, there is another instability in the problem with the reference boundary conditions and that it is related to the instability of the boundary layer at the outlet. For problems considered here, we have not found such instability in the case of the pressure-stress conditions. However, for the converging flows with the pressure-no-slip conditions, for some azimuthal modes (with $n = 3, \dots, 7$), there are three different instability domains (see Fig 14) where instability has different mechanisms: inviscid instability, instability of the boundary layer at the outlet and instability due to the instability of the Couette-Taylor flow discussed above. For the diverging flows with the pressure-no-slip conditions, Figs. 10 and 11 show that the instability domain already covers almost the entire (γ_1, R) plane. Even if there were different mechanisms of instability in different regions of the plane, it would be impossible to identify those regions.

There are many open questions in this area. Here we mention only one, perhaps, the most important question. As was argued in section 3, the pressure-no-slip conditions may be relevant to flow between

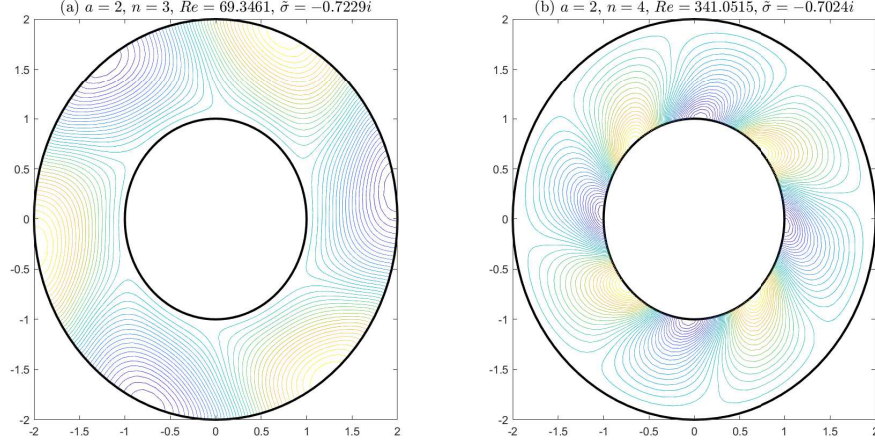


Figure 17: Neutral modes for the Couette-Taylor flow between a rotating impermeable cylinder and a stationary permeable cylinder: (a) the outer cylinder is permeable; (b) the inner cylinder is permeable.

porous cylinders, provided that the pressure in the porous cylinders is known. A more thorough approach would be to consider flows in the free flow domain and in the porous cylinders and match them at the porous walls. A model of this type has been considered by Tilton et al (2010), who have computed a steady viscous flow between a porous cylindrical membrane and an impermeable cylinder with realistic boundary conditions, obtained using Darcy's law for the flow in the membrane. As far as we are aware, there are no results on the stability of steady flows between rotating porous cylinders with realistic boundary conditions, and this is a subject of a continuing investigation.

Acknowledgements. The authors want to thanks Prof. V. A. Vladimirov for helpful discussions. A. Morgulis would like to acknowledge continuing support of the Southern Federal University (Rostov-on-Don).

5 Appendix A

Here we show that the basic steady flows (3.12), (3.13) and (3.12), (3.14) are asymptotically stable to two-dimensional axisymmetric perturbations of arbitrary amplitude. In particular, this means that if $n = 0$, then $\text{Re}(\sigma) < 0$, i.e. the mode with $n = 0$ cannot be unstable.

Let

$$u = \frac{\beta}{r} + \tilde{u}(r, t), \quad v = V_\beta(r) + \tilde{v}(r, t)$$

where $V_\beta(r)$ is given by (3.12), and $\tilde{u}(r, t)$ and $\tilde{v}(r, t)$ represent an axisymmetric perturbation of finite amplitude. Substituting these into Eqs. (3.17), we obtain

$$\begin{aligned} \left(\partial_t + \frac{\beta}{r} \partial_r \right) \tilde{u} - \frac{\beta}{r^2} \tilde{u} - \frac{2V_\beta}{r} \tilde{v} + \tilde{u}\tilde{u}_r - \frac{\tilde{v}^2}{r} &= -\tilde{p}_r + \frac{1}{R} \left(L_0 \tilde{u} - \frac{\tilde{u}}{r^2} \right), \\ \left(\partial_t + \frac{\beta}{r} \partial_r \right) \tilde{v} + \frac{\beta}{r^2} \tilde{v} + \Omega_\beta(r) \tilde{u} + \tilde{u}\tilde{v}_r + \frac{\tilde{u}\tilde{v}}{r} &= \frac{1}{R} \left(L_0 \tilde{v} - \frac{\tilde{v}}{r^2} \right), \\ (r\tilde{u})_r &= 0. \end{aligned}$$

Here \tilde{p} is the perturbation pressure and $L_0 = \partial_r^2 + r^{-1}\partial_r$. The boundary conditions for \tilde{u} at the inlet are $\tilde{u}|_{r=1} = 0$ for the diverging flow ($\beta = 1$) and $\tilde{u}|_{r=a} = 0$ for the converging flow ($\beta = -1$). The

incompressibility condition, together with these boundary conditions for \tilde{u} imply that $\tilde{u} \equiv 0$, so that the first two of the above equations simplify to

$$\begin{aligned} -\frac{2V_\beta}{r} \tilde{v} - \frac{\tilde{v}^2}{r} &= -\tilde{p}_r, \\ \left(\partial_t + \frac{\beta}{r} \partial_r \right) \tilde{v} + \frac{\beta}{r^2} \tilde{v} &= \frac{1}{R} \left(L_0 \tilde{v} - \frac{\tilde{v}}{r^2} \right). \end{aligned} \quad (\text{A1})$$

The second of these is independent from the first one and should be solved subject to appropriate boundary conditions for \tilde{v} , while the first equation can be used to find the pressure \tilde{p} .

In the case of the pressure-no-slip conditions, we have

$$\tilde{v} \big|_{r=1} = 0, \quad \tilde{v} \big|_{r=a} = 0.$$

It had been shown in Ilin & Morgulis (2015) that Eq. (A1) with these boundary conditions has only decaying (with time) solutions. This implies the asymptotic stability.

Consider now the diverging flow ($\beta = 1$) with the pressure-stress conditions, i.e.

$$\tilde{v}(1, t) = 0, \quad \tilde{v}(a, t) - \frac{\tilde{v}(a, t)}{a} = 0. \quad (\text{A2})$$

Let

$$E = \int_1^a \frac{\tilde{v}^2}{2} r dr.$$

The equation of the balance of the perturbation energy, E , can be written as

$$\dot{E} + \frac{\tilde{v}^2}{2} \bigg|_{r=a} + \int_1^a \frac{\tilde{v}^2}{r} dr = -\frac{1}{R} \int_1^a \left(\tilde{v}_r - \frac{\tilde{v}}{r} \right)^2 r dr. \quad (\text{A3})$$

Equation (A3) follows from the following chain of equalities

$$\int_1^a \left(\tilde{v}_r - \frac{\tilde{v}}{r} \right)^2 r dr = -\tilde{v}^2 \big|_{r=a} + \int_1^a \left(\tilde{v}_r^2 + \frac{\tilde{v}^2}{r^2} \right) r dr = -\int_1^a \left(\tilde{v}_{rr} + \frac{\tilde{v}_r}{r} - \frac{\tilde{v}}{r^2} \right) \tilde{v} r dr.$$

[Here we used integration by parts and boundary conditions (A2).]

For the converging flow ($\beta = -1$), the energy balance does not work so well, and we employ the perturbation angular momentum, $\Gamma = r\tilde{v}$. In terms of Γ , Eq. (A1) (with $\beta = -1$) takes the form

$$\left(\partial_t - \frac{1}{r} \partial_r \right) \Gamma = \frac{1}{R} r \left(\frac{1}{r} \Gamma_r \right)_r. \quad (\text{A4})$$

The boundary conditions for $\Gamma(r, t)$ that follow from (3.5) and (3.9) can be written as

$$\Gamma(a, t) = 0, \quad \Gamma_r(1, t) - 2\Gamma(1, t) = 0. \quad (\text{A5})$$

Let

$$M = \int_1^a \frac{\tilde{\Gamma}^2}{2} r dr.$$

After multiplying Eq. (A4) by $r\Gamma$, integrating it from 1 to a in r and performing standard calculations involving integration by parts, we find that

$$\dot{M} = -\frac{1}{R} \int_1^a \Gamma_r^2 r dr - \left(1 + \frac{2}{R} \right) \frac{\Gamma^2(1, t)}{2}. \quad (\text{A6})$$

It can be shown that Eqs. (A3) and (A6) imply the inequalities

$$\frac{\dot{E}}{E} \leq -C^+(a) \quad \text{and} \quad \frac{\dot{M}}{M} \leq -\frac{1}{R} C^-(a),$$

where C^\pm are positive constants that depend on a only. These estimates yield at least exponential decay of all perturbations.

6 Appendix B

Diverging flow. Consider the eigenvalue problem, given by Eqs. (3.24), (3.25), (3.31) and (3.32), in the limit $\gamma_1 \rightarrow \infty$. It follows from Eqs. (3.12) and (3.16) with $\beta = 1$ that

$$V(r) = \gamma_1 V_0(r), \quad V_0(r) = -\frac{r^{R+1}}{a^{R+2} - 1} + \frac{a^{R+1}}{a^{R+2} - 1} \frac{1}{r} + O\left(\gamma_1^{-1}\right). \quad (\text{B1})$$

Let

$$\sigma = \gamma_1 \tilde{\sigma}. \quad (\text{B2})$$

Substitution of (B1) and (B2) into Eq. (3.24) yields

$$\left(\tilde{\sigma} + \frac{inV_0}{r}\right) L\hat{\psi} - \frac{in}{r} \Omega'_0(r) \hat{\psi} = \frac{1}{Re} L^2 \hat{\psi} + O\left(\gamma_1^{-1}\right) \quad (\text{B3})$$

where Re is the azimuthal Reynolds number defined by Eq. (3.35).

Now we make our key assumption that is consistent with the behaviour of critical curves in Figs. 10–12, namely: $Re = O(1)$ as $\gamma_1 \rightarrow \infty$. With this assumption, the above formula for $V_0(r)$ simplifies to

$$V_0(r) = \frac{1}{a^2 - 1} \left[\frac{a^2}{r} - r \right] + O\left(\gamma_1^{-1}\right). \quad (\text{B4})$$

Note that if we discard the $O(\gamma_1^{-1})$ term in (B4), then $V_0(r)$ is the same as the azimuthal velocity profile of the classical Couette-Taylor flow between rotating cylinders with radii 1 and a in a particular case where the outer cylinder does not rotate, and the inner cylinder rotates with angular velocity equal to 1.

On substituting (B4) into Eq. (B3), we find that, at leading order,

$$\left(\tilde{\sigma} + \frac{in}{a^2 - 1} \left[\frac{a^2}{r^2} - 1 \right]\right) L\hat{\psi} = \frac{1}{Re} L^2 \hat{\psi}. \quad (\text{B5})$$

At leading order, boundary condition (3.25), (3.31) and (3.32) take the form

$$\hat{\psi}(1) = 0, \quad \hat{\psi}'(1) = 0, \quad \hat{\psi}'(a) = 0, \quad (\text{B6})$$

$$\frac{1}{Re} \left(\hat{\psi}'''(a) + \frac{1}{a} \hat{\psi}''(a) + \frac{4n^2}{a^3} \hat{\psi}(a) \right) - \frac{2in}{a(a^2 - 1)} \hat{\psi}(a) = 0. \quad (\text{B7})$$

Thus, we have obtained the eigenvalue problem for $\tilde{\sigma}$. It was solved numerically using the same method as the original eigenvalue problem. We found that each azimuthal mode becomes unstable for Re greater than some critical value Re_{cr} . The critical azimuthal Reynolds numbers for $a = 2, 8$ and $n = 1, \dots, 5$ are shown in table 1. Using these and formula (3.34), we plotted the asymptotic R_{cr} as a function of γ_1 in Fig. 13 (dashed curves).

Now let us discuss the connection of this result with the classical Couette-Taylor flow. Evidently, if boundary condition (B7) were replaced by the condition $\hat{\psi}(a) = 0$ (i.e. no normal flow at $r = a$), this eigenvalue problem would coincide with the one arising in the particular case of the classical Couette-Taylor flow mentioned above. It is known that the Couette-Taylor flow is linearly stable to two-dimensional

	$a = 2$					$a = 8$				
n	1	2	3	4	5	1	2	3	4	5
Re_{cr}	147.29	77.58	69.35	117.36	188.80	12.54	51.79	100.48	165.39	246.62

Table 1: $Re_{cr}(a, n)$

perturbations, although there seems to be no formal proof of this fact (see, e.g. Drazin & Reid , 1981). However, with boundary condition (B7), the same flow can be unstable. Recalling that the physical meaning of condition (B7) is that the normal stress applied to the fluid at $r = a$ is zero, we conclude that the Couette-Taylor flow with the normal stress condition at the outer cylinder (instead of the normal velocity condition) is unstable to two-dimensional perturbations provided that

$$Re > \min_{n \in \mathbb{N}} Re_{cr}(a, n).$$

Converging flow. Consider the eigenvalue problem, given by Eqs. (3.24), (3.26), (3.31) and (3.33), in the limit $\gamma_2 \rightarrow \infty$. The same arguments as for the diverging flow yield, at leading order, the following eigenvalue problem for $\tilde{\sigma} = \sigma/\gamma_2$:

$$\left(\tilde{\sigma} + \frac{in}{a^2 - 1} \left[1 - \frac{1}{r^2} \right] \right) L\hat{\psi} = \frac{1}{\tilde{Re}} L^2 \hat{\psi}, \quad (B8)$$

$$\hat{\psi}(a) = 0, \quad \hat{\psi}'(a) = 0, \quad \hat{\psi}'(1) = 0, \quad (B9)$$

$$\frac{1}{\tilde{Re}} \left(\hat{\psi}'''(1) + \hat{\psi}''(1) + 4n^2 \hat{\psi}(1) \right) + \frac{2in}{a^2 - 1} \hat{\psi}(1) = 0. \quad (B10)$$

Solving this problem numerically, we find that azimuthal modes with $n = 4, \dots, 9$ become unstable for \tilde{Re} greater than some critical value \tilde{Re}_{cr} . The critical azimuthal Reynolds numbers for $a = 2$ and $n = 4, \dots, 9$ are shown in table 2.

n	4	5	6	7	8	9
\tilde{Re}_{cr}	341.05	546.34	793.46	1093.4	1444.3	1845.7

Table 2: $\tilde{Re}_{cr}(a, n)$ for $a = 2$

References

- ANDERECK, C.D., LIU, S.S. AND SWINNEY, H.L. 1986 FLOW REGIMES IN A CIRCULAR COUETTE SYSTEM WITH INDEPENDENTLY ROTATING CYLINDERS, *J. FLUID MECH.*, **164**, 155–183.
- ANTONTSEV, S. N., KAZHIKHOV, A. V. AND MONAKHOV, V. N. 1990 BOUNDARY VALUE PROBLEMS IN MECHANICS OF NONHOMOGENEOUS FLUIDS [TRANSLATED FROM THE RUSSIAN]. *STUDIES IN MATHEMATICS AND ITS APPLICATIONS*, VOL. 22, NORTH-HOLLAND PUBLISHING CO., AMSTERDAM, 309 pp.
- BAHL, S. K. 1970 STABILITY OF VISCOUS FLOW BETWEEN TWO CONCENTRIC ROTATING POROUS CYLINDERS, *DEF. SCI. J.*, **20**(3), 89–96.
- BEADOIN, G. AND JAFFRIN, M. Y. 1989 PLASMA FILTRATION IN COUETTE FLOW MEMBRANE DEVICES, *ARTIF. ORGANS*, **13**(1), 43–51.
- BEAVERS, G. S. AND JOSEPH, D. D. 1967 BOUNDARY CONDITIONS AT A NATURALLY PERMEABLE WALL, *J. FLUID MECH.*, **30**(1), 197–207.

- CHOSSAT, P. AND IOOSS, G. 1994 THE COUETTE-TAYLOR PROBLEM. *APPLIED MATHEMATICAL SCIENCES*, VOL. 102. SPRINGER, NEW YORK, 233 PP.
- DRAZIN, P. G. AND REID, W. H. 1981 HYDRODYNAMIC STABILITY. CAMBRIDGE UNIVERSITY PRESS.
- Fujita, H., Morimoto, H. and Okamoto, H. 1997 Stability analysis of Navier-Stokes flows in annuli, *Mathematical methods in the applied sciences*, **20**(11), 959–978.
- GALLAIRE, F. AND CHOMAZ, J.-M. 2004 THE ROLE OF BOUNDARY CONDITIONS IN A SIMPLE MODEL OF INCIPIENT VORTEX BREAKDOWN, *PHYS. FLUIDS*, **16**(2), 274–286.
- GALLET, B., DOERING, C. R. AND SPIEGEL, E. A. 2010 DESTABILIZING TAYLOR-COUETTE FLOW WITH SUCTION, *PHYS. FLUIDS*, **22**(3), 034105.
- GIORDANO, R. C., GIORDANO, R. L. C., PRAZEREST, D. M. F. AND COONEY, C. L. 1998 ANALYSIS OF A TAYLOR-POISEUILLE VORTEX FLOW REACTOR-I: FLOW PATTERNS AND MASS TRANSFER CHARACTERISTICS, *CHEMICAL ENGINEERING SCIENCE*, **53**(20), 3635–3652.
- GOTTLIEB, D. AND ORSZAG, S. A. 1977 NUMERICAL ANALYSIS OF SPECTRAL METHODS: THEORY AND APPLICATIONS. CBMS-NSF REGIONAL CONFERENCE SERIES IN APPLIED MATHEMATICS, SIAM, PHILADELPHIA.
- GRESHO, P. M. 1991 INCOMPRESSIBLE FLUID DYNAMICS: SOME FUNDAMENTAL FORMULATION ISSUES. *ANNUAL REVIEW OF FLUID MECHANICS*, **23**, 413–531.
- GUADAGNI, S., GIACHI, M., FUSI, L. AND FARINA, A. 2020 FLOW STABILITY IN A WIDE VANELESS DIFFUSER, *APPLICATIONS IN ENGINEERING SCIENCE*, **4**, 100025.
- GUNZBURGER, M.D. 1989 FINITE ELEMENT METHODS FOR VISCOUS INCOMPRESSIBLE FLOWS: A GUIDE TO THEORY, PRACTICE, AND ALGORITHMS. BOSTON: ACADEMIC.
- HABER, S. AND MAURI, R. 1983 BOUNDARY CONDITION FOR DARCY’S FLOW THROUGH POROUS MEDIA, *INT. J. MULTIPHASE FLOW*, **9**(5), 561–574.
- HEYWOOD, J. G., RANNECHER, R. AND TUREK, S. 1996 ARTIFICIAL BOUNDARIES AND FLUX AND PRESSURE CONDITIONS FOR THE INCOMPRESSIBLE NAVIER-STOKES EQUATIONS, *INT. J. NUM. METH. FLUIDS*, **22**, 325–352.
- ILIN, K. 2008 VISCOUS BOUNDARY LAYERS IN FLOWS THROUGH A DOMAIN WITH PERMEABLE BOUNDARY. *EUR. J. MECH. B/FLUIDS*. **27**, 514–538.
- ILIN, K. AND MORGULIS, A. 2013 INSTABILITY OF AN INVISCID FLOW BETWEEN POROUS CYLINDERS WITH RADIAL FLOW, *J. FLUID MECH.*, **730**, 364–378.
- ILIN, K. AND MORGULIS, A. 2015 INSTABILITY OF A TWO-DIMENSIONAL VISCOUS FLOW IN AN ANNULUS WITH PERMEABLE WALLS TO TWO-DIMENSIONAL PERTURBATIONS, *PHYS. FLUIDS*, **27**, 044107.
- ILIN, K. AND MORGULIS, A. 2017 INVISCID INSTABILITY OF AN INCOMPRESSIBLE FLOW BETWEEN ROTATING POROUS CYLINDERS TO THREE-DIMENSIONAL PERTURBATIONS, *EUR. J. MECH. - B/FLUIDS*, **62**(1), 46–60.
- ILIN, K. & MORGULIS, A. 2020 ON THE STABILITY OF THE COUETTE-TAYLOR FLOW BETWEEN ROTATING POROUS CYLINDERS WITH RADIAL FLOW, *EUR. J. MECH. - B/FLUIDS*, **80**(1), 174–186.
- Johnson, E. C. and Lueptow, R. M. 1997 Hydrodynamic stability of flow between rotating porous cylinders with radial and axial flow, *Phys. Fluids*, **9**(12), 3687–3696.

- KAZHIKHOV, A.V. AND RAGULIN, V.V. 1983 FLOW PROBLEM FOR THE EQUATIONS OF AN IDEAL FLUID, *J. MATH. SCI.*, **21**, 700–710. [TRANSLATED FROM ZAPISKI NAUCHNYKH SEMINAROV LENINGRADSKOGO OTDELENIYA MATEMATICHESKOGO INSTITUTA IM. V. A. STEKLOVA AKAD. NAUK SSSR, VOL. 96, PP. 84-96, 1980.]
- KERSALE, E., HUGHES, D. W., OGILVIE, G. I., TOBIAS, S. M. AND WEISS, N. O. 2004 GLOBAL MAGNETOROTATIONAL INSTABILITY WITH INFLOW, I. LINEAR THEORY AND THE ROLE OF BOUNDARY CONDITIONS, *ASTROPHYS. J.*, **602**(2), 892–903.
- KERSWELL, R. R. 2015 INSTABILITY DRIVEN BY BOUNDARY INFLOW ACROSS SHEAR: A WAY TO CIRCUMVENT RAYLEIGH’S STABILITY CRITERION IN ACCRETION DISKS? *J. FLUID MECH.*, **784**, 619–663.
- KOLESOV, V. AND SHAPAKIDZE, L. 1999 ON OSCILLATORY MODES IN VISCOUS INCOMPRESSIBLE LIQUID FLOWS BETWEEN TWO COUNTER-ROTATING PERMEABLE CYLINDERS, IN: *TRENDS IN APPLICATIONS OF MATHEMATICS TO MECHANICS* (ED. G. IOOSS, O. GUES & A NOURI), CHAPMAN AND HALL/CRC, PP. 221–227.
- KOLYSHKIN, A. A. AND VAILLANCOURT, R. 1997 CONVECTIVE INSTABILITY BOUNDARY OF COUETTE FLOW BETWEEN ROTATING POROUS CYLINDERS WITH AXIAL AND RADIAL FLOWS. *PHYS. FLUIDS* **9**, 910–918.
- LJEVAR, S., LANGE, DE, H. C. AND STEENHOVEN, VAN, A. A. (2006) COMPARISON OF A TWO-DIMENSIONAL VISCID AND INVISCID MODEL FOR ROTATING STALL ANALYSIS, *PROCEEDINGS OF THE 4TH WSEAS INTERNATIONAL CONFERENCE ON FLUID MECHANICS AND AERODYNAMICS, ELOUNDA, GREECE, AUGUST 21-23, 2006*, 376–383 (AVAILABLE ONLINE: [HTTP://WWW.WSEAS.US/E-LIBRARY/CONFERENCES/2006ELOUNDA2/PAPERS/538-127.PDF](http://www.wseas.us/e-library/conferences/2006elounda2/papers/538-127.pdf)).
- MARTINAND, D., SERRE, E. AND LUEPTOW, R. M. 2009 ABSOLUTE AND CONVECTIVE INSTABILITY OF CYLINDRICAL COUETTE FLOW WITH AXIAL AND RADIAL FLOWS, *PHYS. FLUIDS*, **21**(10), 104102.
- MARTINAND, D., SERRE, E. AND LUEPTOW, R. M. 2017 LINEAR AND WEAKLY NONLINEAR STABILITY ANALYSES OF CYLINDRICAL COUETTE FLOW WITH AXIAL AND RADIAL FLOWS, *J. FLUID MECH.*, **824**, 438–476.
- MIN, K. AND LUEPTOW, R. M. 1994 HYDRODYNAMIC STABILITY OF VISCOUS FLOW BETWEEN ROTATING POROUS CYLINDERS WITH RADIAL FLOW, *PHYS. FLUIDS*, **6**(1), 144–151.
- MORGULIS, A. B. AND YUDOVICH, V. I. 2002 ARNOLD’S METHOD FOR ASYMPTOTIC STABILITY OF STEADY INVISCID INCOMPRESSIBLE FLOW THROUGH A FIXED DOMAIN WITH PERMEABLE BOUNDARY, *CHAOS*, **12**, 356–371.
- SAFFMAN, P. G. 1971 ON THE BOUNDARY CONDITION AT THE SURFACE OF A POROUS MEDIUM, *STUDIES IN APPLIED MATHEMATICS*, **52**(2), 93–101.
- SERRE, E., SPRAGUE, M. A. AND LUEPTOW, R. M. 2008 STABILITY OF TAYLOR-COUETTE FLOW IN A FINITE-LENGTH CAVITY WITH RADIAL THROUGHFLOW, *PHYS. FLUIDS*, **20**(3), 034106.
- TEMAM, R. AND WANG, X. 2000 REMARKS ON THE PRANDTL EQUATION FOR A PERMEABLE WALL. *Z. ANGEW. MATH. MECH.*, **80**, 835–843.
- TSUJIMOTO, Y., YOSHIDA, Y. AND MORI, Y. 1996 STUDY OF VANELESS DIFFUSER ROTATING STALL BASED ON TWO-DIMENSIONAL INVISCID FLOW ANALYSIS. *ASME J. FLUIDS ENGINEERING*, **118**, 123–127.
- TILTON, N., MARTINAND, D., SERRE, E. AND LUEPTOW, R. M. 2010 PRESSURE-DRIVEN RADIAL FLOW IN A TAYLOR-COUETTE CELL, *J. FLUID MECH.*, **660**, 527–537.

WROŃSKI, S., MOLGA, E. AND RUDNIAK, L. 1989 DYNAMIC FILTRATION IN BIOTECHNOLOGY, *BIOPROCESS ENGINEERING*, **4**(3), 99–104.

YUDOVICH, V.I. 2001 ROTATIONALLY SYMMETRIC FLOWS OF INCOMPRESSIBLE FLUID THROUGH AN ANNULUS. PARTS 1 AND 2. PREPRINTS VINITI NO. 1862-B01 AND 1843-B01 (IN RUSSIAN).